Fabrication of Short Polymer Fibers by Electrospinning and Control of Fiber Length

(静電紡糸法によるポリマー短繊維の合成および繊維長の制御)

By

Indra Wahyudhin Fathona

HIROSHIMA UNIVERSITY

SEPTEMBER 2014

Fabrication of Short Polymer Fibers by Electrospinning and Control of Fiber Length
(静電紡糸法によるポリマー短繊維の合成および繊維長の制御)

A Dissertation Submitted to
The Department of Chemical Engineering
Graduate School of Engineering
Hiroshima University

By
Indra Wahyudhin Fathona

In Partial Fulfillment of the Requirement

For the Degree of

Doctor of Engineering

Hiroshima University

July 2014

Approved by

Professor Akihiro Yabuki

Advisor

Acknowledgement

First, I would like to express my praise and gratitude to Allah the almighty for the gifts and blessings. I would like to express my sincere gratitude to Professor Akihiro Yabuki for his guidance, support, and patience during my doctoral study. I also would like to express my sincere gratitude to Professor Okuyama for all support since the beginning to the end of my program. They also give me a precious chance to get doctoral degree in Hiroshima University.

I wish thank to Professor Sakohara Syuuji and Professor Shiono Takeshi for their patience, wisdom, and the valuable comments and suggestion. My grateful thank also dedicated to Dr. Takashi Ogi and Dr. Toru Iwaki for their great support, advice, and guidance during my research.

Special thanks are spent to Professor Khairurrijal, Professor Mikrajuddin Abdullah, Dr. Ferry Iskandar, and Dr. Muhammad Miftahul Munir, Department of Physics Institut Teknologi Bandung, for theirs never ending support on research discussion and inspired spirit and work ethic, I am so proud to be theirs student and collage. I also thanks to Dr. Asep Bayu Dani Nandiyanto, Dr. Asep Suhendi, and all members of Thermal-Fluid Engineering Laboratory for theirs help and kindness in daily life.

Thanks to Ministry of Education, Culture, Sports, Science and Technology (MEXT) of japan for providing a doctoral scholarship, and Graduate School of Engineering of Hiroshima University, Japan for organizing a doctoral course.

I would to thank to my beloved wife and daughter, to my parents, sister, and brother for theirs support, pray, patience, motivation, and sacrifice. They give immeasurable things into my life, and brought me happiness when I was down. Theirs love give me a power and spirit to finish my study well.

Indra Wahyudhin Fathona

Higashi Hiroshima, July 2014

Abstract

Polymer nanofibers are commonly fabricated by electrospinning methods for application such as affinity membranes, filter media, and electrical application, etc. Short polymer fibers have certain length, in which reliable as filler in composite materials, drugs carrier, and material template. In this dissertation, two types of one-step fabrication processes for short polymer fibers by electrospinning were developed, which is used electric spark as cutting tool and is controlled electrospinning conditions. The methodology to control the length of short polymer fibers was developed by altering a needle inner diameter, applied voltage, flow rate of polymer solution, and added the nanoparticles.

Chapter 1 provides an introduction and current progress of various methods to fabricate polymer fibers, which are drawing method, template synthesis, phase separation, self-assembly, and electrospinning.

Chapter 2 describes a development of one-step electrospinning process by electric spark as a cutting tool to fabricate short electrospun polymer fibers. A solution of cellulose acetate and organic solvent was ejected from a syringe needle and was stretched by the electric field then it cut after passed through the gap between the tips of two electrodes that generated an electric spark with frequency of 5 kHz. The obtained short fibers have average length of 231 μm, and the theoretical calculation of fiber length has been developed based on solution flow rate and electric spark frequency, which fit with the experimental data.

Chapter 3 describes a simple one-step fabrication of short elcectrospun polymer nanofibers with controllable length by manipulating polymer concentration, flow rate, and applied voltage. The concentration of the cellulose acetate polymer in the

solution was important factor which varied from 13 to 15 wt. %. The length of fibers was increased by increasing the flow rate of the solution, and it was decreased with an increase in applied voltage, resulting in controllable length of short nanofibers at 37 to 670 μm. The polymer solution jet ejected straight from the needle tip then it split and segmented into short fiber because of the rapid increase of the repulsive force from surface charges combined longitudinal forces from the applied voltage.

Chapter 4 describes the effect of inner diameter of a needle on the length of electrospun polymer fibers. Cellulose acetate solution was ejected from various needles with different inner diameter then it split and breaks into short polymer fibers by electrostatic repulsion. The length could be controlled from 10 to 240 μm by increasing the inner diameter of needle from 0.11 to 0.26 mm.

Chapter 5 describes the fabrication of short composite nanofibers of TiO_2/cellulose acetate. The length of the short composite nanofibers was significantly decreased from 112 to 70 μm by the addition of 5 wt. % concentration of nanoparticles, and it gradually continued to decrease as the nanoparticle concentration was increased to 50 wt. %. The length of the short composite nanofibers with a low concentration of nanoparticles was affected by the surface charge of the nanoparticles, and negatively charged nanoparticles readily dispersed to the negatively charged polymers in solution, which resulted in an elongation of the fabricated short composite nanofibers.

Chapter 6 describes a summary and some comments for further investigations.

Contents

List of Figures

Chapter 1

Introduction

1.1. Background

Polymer fiber with diameter ranging from nanometer to micrometer is of great interest because of their unique properties and has applications in many areas. They have advantages and outstanding properties compared with their bulk size [1]. The term of polymer micro-fiber is used to describe the polymer fiber with diameter ranging from 1-100 μm, whereas the term of nanofiber is used to describe the polymer fiber with a diameter less than 1 μm. As the diameter of fiber shrunk from micrometer to nanometer, the surface area to volume ratio of fiber was increased resulting in the changing on physical properties [1]. Polymeric fibers can be produced with different morphologies such as beaded fiber, short fiber, continuous fiber, and coaxial fiber morphologies in which each has different applications. Therefore, control over the fiber morphology is dispensable for their applications [2-6].

Several researchers have reported various morphologies of polymeric fibers, such as beaded fibers, coaxial fiber, and short fibers [7-13]. Beaded fiber describes as a continuous fiber with beads along its body. The occurrence of beads was causing the lack of diameter uniformity. Beaded fiber can be fabricated by electrospinning by altering the concentration of polymer in the precursor solution applied voltage, and altering the additional ion on the precursor solution [7]. Coaxial fiber has a core-sheath structure with core part consist of several channels and can be fabricated by eletrsopinning method. This structure allows the formation of the hollow fiber and also

allows the encapsulation of several materials within the fiber [8]. Coaxial beaded fiber has been applied as container of self-healing coating on the metal substrate [14].

Recently, short fiber fabrication has been a hot topic due to its wide applications in the aerospace industry, automotive industry, corrosion protection, flexible display, etc. [15-18]. Short fiber is a discrete fiber with lengths varied several nanometer to a few millimeters. Short fiber fabrication can be done with one process or multiple processes. In general, short-fiber fabrication is done by two processes, where the second process is a process of cutting the continuous fiber into short fiber. The technique used is the injection molding and extrusion in which the cutting is done mechanically with a knife to make a short fiber [19-20]. Short fibers can also be made by electrospinning by using mechanically and chemically cutting methods as a secondary process which performed on continuous electrospun fiber to obtain short fiber [12,13]. However, the short fiber fabrication by multiple processes has some deficiencies that cause the process becomes inefficient and effective. Therefore, in this doctoral program, we are interesting in developing a one-step process of short fiber fabrication by electrospinning.

In this dissertation, two types of one-step fabrication processes for short polymer fibers by electrospinning were developed, which is used electric spark as cutting tool and is controlled electrospinning conditions. The methodology to control the length of short polymer fibers was developed by altering a needle inner diameter, applied voltage, flow rate of polymer solution, and added the nanoparticles.

1.2. Fabrication methods of short polymer fiber

There are a number of techniques to fabricate short polymeric fiber, such as drawing, template synthesis, self-assembly, and electrospinning, which resulted in the

polymer fiber with diameter varied from several nanometer to micrometer and length varied from several nanometers to meters [21]. These short polymer fibers have been applied as a sensor, drug delivery system, corrosion self-healing, membrane, etc.

1.2.1. Drawing method

The drawing method can produce fine fiber with diameter ranging from 2 to 100 nm and length ranging from 10 μm to several millimeters. Commonly, a sodium citrate dissolve in chloroauric acid is use as a precursor solution. The milimetric droplet of precursor solution is deposited on the surface and the fiber is fabricated by dipping a micropipette into a milimetric droplet then withdrawn at speed of approximately 10^{-4} ms^{-1}[21]. The viscoelasticity of milimetric droplet is an important factor in drawing method that can undergo strong deformation while being cohesive enough to support the stress developed during the pulling. While using the polymer material as a precursor solution, the length of obtained fiber were elongated due to the high molecular weight of polymer materials increase viscoelasticity of the drawing solution [22,23]. The advantage of drawing method is requiring minimum equipment, whereas the disadvantage is discontinuous process. The length of short polymer fiber fabricated by this method is depend on the viscoelasticity and viscosity of used polymer that correlate with the tensile strength of polymer.

1.2.2. Template synthesis method

The template synthesis is a method to fabricate fiber by using a metal oxide membrane as a template or mold. Commonly, nanoporous aluminum oxide is utilized as a membrane. This method can fabricate fiber with length 10 μm and fiber diameter can

be adjusted by altering the pores sizes of membrane. The fibers are fabricate within the single column chamber consist of water, polymer solution, membrane, and solidification solution, which the solidification solution is separated from water and polymer solution by aluminum oxide membrane. Pressurized water pushes the polymer solution into a nanoporous membrane then the polymer fibers are come out from the nanoporous membrane and solidified after contact with solidification solution. The advantage of this method is the diameter of fiber can be adjusted by altering the template size [21,24].

1.2.3. Self-assembly method

The fabrication of short polymer fiber by self-assembly method is performed by assembling the smaller molecules as building blocks into the nano-scale fiber. The diameter of fiber is 7-100 nm and length varied from 1-20 μm [25-27]. The important factor in fiber formation is intermolecular forces that caused the smaller units stick together and the molecular shape that determine the shape of macromolecular shape. This technique is feasible for fabrication of smaller polymeric fiber. However, it has disadvantages such as take complex processes.

1.2.4. Electrospinning method

Electrospinning is the simplest and most reliable technique to fabricate polymer fibers, which use high electric voltage. The conventional setup of electrospinning is consist of a syringe with metal needle to hold the polymer solution, a syringe pump to drain out the polymer solution through the tip of metal needle, a DC voltage power supply in kV range, and grounded collector plate. High voltage is applied to a viscous polymer solution in order to create an electrified polymer solution jet. The jet is

continuously stretched by electrostatic repulsions between the surface charges and the solvent is evaporated leaving behind the polymer fiber [2].

Commonly, continuous fibers with diameter varied from 3 nm to 1 μm were obtained by electrospinning method. The morphology of fiber such as smooth fiber and beaded fiber is affected by polymer chain entanglement, which correlated directly with polymer concentration in the solution. The polymer solution with chain entanglement between 1 and 2.5 will produce beaded fiber, whereas polymer solution with chain entanglement more than 2.5 will produce smooth and continuous fiber [28,29]. Electrospinning method also can fabricate coaxial fiber by utilizing coaxial needle or single needle. Polymer/polymer or polymer/oil is utilized as an inner and outer solution while the coaxial needle is used to fabricate coaxial fiber [30-33], whereas the emulsion of polymer /polymer solution is used as precursor solution while the single needle is used [33]. Composite polymer fiber is another type of fiber that can be produced by electrospinning method. The precursor solution for electrospinning is a suspension of polymer/nanoparticles [34-36].

Short polymer fiber can be fabricated by one-step process of electrospinning or multiple processes. Luo et al reported the one-step fabrication of short fiber by electrospinning [9]. The different molecular weight of polymethylsilsesquioxane polymer were dissolve in the volatile solvent resulted in short microfiber with aspect ratio varied from 10-200. The length of fiber was affected by molecular weight of polymer therefore to control the length of fiber was not easy. The fabrication of short polymer fiber by multiple processes including electrospinning is reported by several researchers. Cutting process of continuous electrospun as a post processing is necessary in order to obtain short fiber. A UV cutting method has been employed by Stoiljkovic

and Agarwal to produce 20-150 μm fibers [12]. They employed the concept of a photocross-linking reaction upon UV radiation. The precursor for electrospinning was double bound polymers with a photocross-linker and a photoinitiator. The electrospun fibers were irradiated by UV in the presence of a mask slit, and, thus, the uncovered fibers were cross-linked and insoluble, whereas the covered fibers were non-cross-linked and soluble in the appropriate solvent. The short fibers were obtained by immersing the irradiated fibers into the appropriate solvent. However, the length of the fibers was limited by the width of the mask, and the process took more than one step. Yoshikawa et al. reported the fabrication of shortened electrospun polymer fibers with a well-defined concentrated polymer brush [13]. First, the electrospun fibers were fabricated by electrospinning then the brush was formed on the surface of electrospun fibers by atom transfer radical polymerization. The short fibers were obtained by cutting the dispersed fibers in the water using homogenizer for 1 to 3h. The short fibers cut by the Yoshikawa method were 11 μm in length and controllable by adjusting the cutting time in the water. However, this technique requires several steps and much time for the polymerization and cutting of the fibers. The current cutting methods are not entirely convenient and require a relatively long amount of time due to the secondary process, therefore a simple and straight-forward cutting method is necessary.

1.3. Objectives and outline of dissertation

The objective of this dissertation is to investigate the fabrication of short polymer fibers by electrospinning and controlling electrospinning parameter in order to obtain the controlled length of polymer fiber. Two types of one-step fabrication processes for short polymer fibers by electrospinning were developed, which is used

electric spark as cutting tool and is controlled electrospinning conditions. The methodology to control the length of short polymer fibers was developed by altering a needle inner diameter, applied voltage, flow rate of polymer solution. The effect of nanoparticles and theirs surface charge on the length of composite fiber were also investigated. Cellulose acetate solution is used as precursor for short fiber fabrication. The background and review of polymer fiber fabrication is describes in Chapter 1 and outline of this dissertation is shown in **Figure 1**.

Chapter 2 describes a development of one-step electrospinning process by electric spark as a cutting tool to fabricate short electrospun polymer fibers. A solution of cellulose acetate and organic solvent was ejected from a syringe needle and was stretched by the electric field then it cut after passed through the gap between the tips of two electrodes that generated an electric spark with frequency of 5 kHz. The short fibers were found on the collector plate with a density of 1-5 fibers per 0.12x0.2 mm^2, whereas the fibers that did not flow through to the electric spark were uncut and remained as continuous fibers on the collector plate. The continuous fibers were dominant on the collector plate due to the limited size of the cutting area of the electric spark: 1.5x0.5 mm^2. The theoretical fiber length was calculated from the flow rate and the cross-sectional area of the precursor polymer solution fibers, and the damped oscillation frequency of the electric spark. The theoretical fiber length was calculated at 271 μm when employing a 5 kHz of electric spark, which was in good agreement with the length of the short fibers obtained in the experiment.

Chapter 3 describes the fabrication of elcectrospun short polymer nanofibers with controllable length by manipulating polymer concentration and processing parameters such as solution flow rate and voltage. The conventional electrospinning

setup is used and the production rate of short fiber is higher than that of electric spark cutting method. The concentration of the cellulose acetate polymer in the solution was important factor which varied from 13 to 15 wt. %. The length of fibers was increased by increasing the flow rate of the solution, and it was decreased with an increase in applied voltage, resulting in controllable length of short nanofibers at 37 to 670 µm. The polymer solution jet ejected straight from the needle tip then it split and segmented into short fiber because of the rapid increase of the repulsive force from surface charges combined longitudinal forces from the applied voltage. The breaking of the fibers into short nanofibers occurred because the repulsive force from the surface charges and the longitudinal force from the applied voltage surpassed the tensile strength of the polymer solution jet.

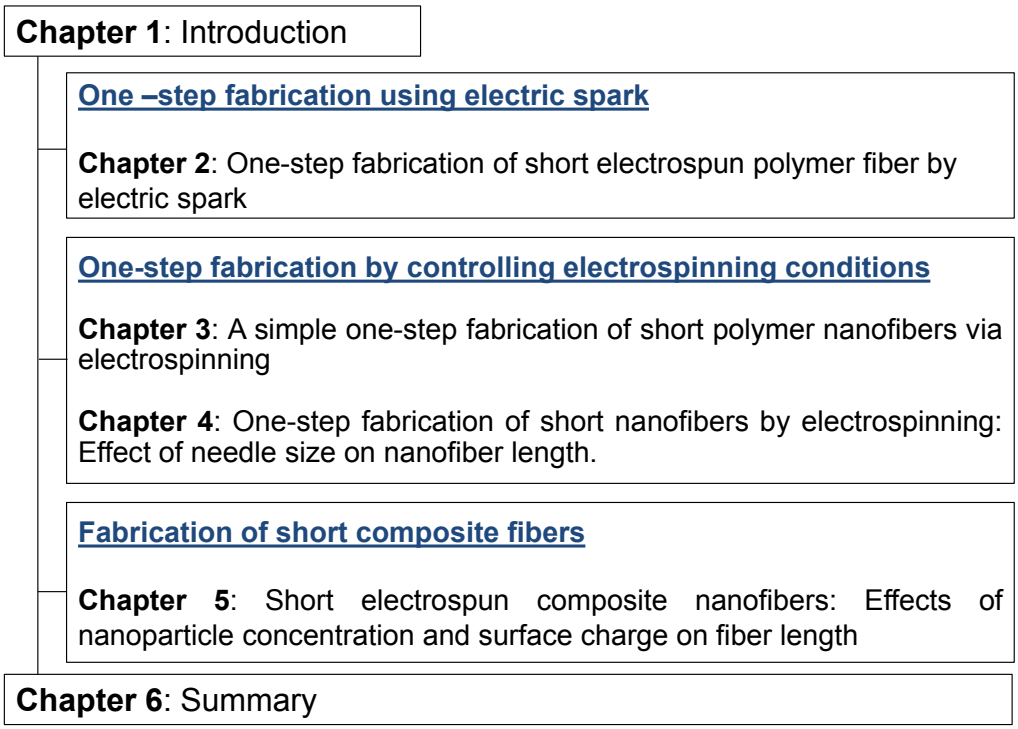

Figure 1. Dissertation outline

Chapter 4 describes a study of the needle inner diameter effect on the fiber length. Cellulose acetate solution was ejected from various needles with different inner diameter then it split and break into short polymer fibers by electrostatic repulsion. The length of electrospun polymer fiber could be controlled from 10-240 μm by increasing the inner diameter of needle from 0.11 to 0.26 mm.

Chapter 5 describes the fabrication of short composite nanofiber of TiO2/cellulose acetate. The length of the short composite nanofibers was significantly decreased from 112 to 70 μm by the addition of 5 wt. % concentration of nanoparticles, and it gradually continued to decrease as the nanoparticle concentration was increased to 50 wt. %. The length of the short composite nanofibers with a low concentration of nanoparticles was affected by the surface charge of the nanoparticles, and negatively charged nanoparticles readily dispersed to the negatively charged polymers in solution, which resulted in an elongation of the fabricated short composite nanofibers.

In Chapter 6, the summary of all chapters is presented.

1.4. References

[1] Z.M. Huang, Y.Z. Zhang, M. Kotaki, S. Ramakrishna, A review on polymer nanofiber by electrospinning and their applications in nanocomposites, Composites Sci. Technol. 63 (2003) 2223-2253.

[2] D. Li, Y. Xia, Electrospinning of nanofibers: reinventing the wheel?, Adv. Mater 16 (2004) 1151-1170.

[3] H. Fong, I. Chun, D.H. Reneker, Beaded nanofiber form during electrospinning, Polymer 40 (1999) 4585-4592.

[4] J.M. Deitzel, K.K. Meyer, D. Harris, N.C.B. Tan, The effect of processing variables on the morphology of electrospun nanofibers and textiles, Polymer 42 (2001) 261-272.

[5] H. Fong, W. Liu, C.S. Wang, R.A. Vaia, Generation of electrospun fibers of nylon 6 and nylon 6-montmorillonite nanocomposite, Polymer 43 (2002) 775- 780.

[6] M.G. McKee, G.L. Wilkes ,R.H. Colby, T.E. Long, Correlations of solution rheology with electrospun fiber formation of linear and branched polyesters, Macromol. 37 (2004) 1760-1767.

[7] K.H. Lee, H.Y. Kim, H.J. Bang, Y.H. Jung, SG Lee, The change of bead morphology formed on electrospun polystyrene, Polymer 44 (2003) 4029-4034.

[8] Z. Sun, E. Zussman, A.L. Yarin, J.H. Wendorff and A. Greiner, Compound core–shell polymer nanofibers by co-electrospinning, Adv. Mater. 15 (2003) 1929-1932.

[9] C.J. Luo, E. Stride, S. Stoyanov, E. Pelan, M. Edirisinghe, Electrospinning short polymer micro-fibres with average aspect ratios in the range of 10-200, J Polym. Res. 18 (2011) 2515-2522.

[10] I.W. Fathona, A. Yabuki, One-step fabrication of short electrospun fibers using an electric spark, J. Mater. Proces. Technol. 213 (2013) 1894-1899.

[11] I.W. Fathona, A. Yabuki, A Simple One-Step Fabrication of Short Polymer Nanofibers via Electrospinning, J. Mater. Sci. 49 (2014) 3519-3528.

[12] A. Stoiljkovic, S. Agarwal, Short electrospun fibers by UV cutting method, Macromol. Mater. Eng. 293 (2008) 895-899.

[13] C. Yoshikawa, K. Zhang, E. Zawadzak, and H. Kobayashi, A novel shortened electrospun nanofiber modified with a ‘concentrated’ polymer brush, Sci. Technol. Adv. Mater. 12 (2011) 1-7.

[14] J.H. Park, P.V. Braun, Coaxial electrospinning of self-healing coating, Adv. Mater. 22 (2010) 496-499.

[15] L.N. Song, M. Xiao, X.H. Li, Y.Z. Meng, Short carbon fiber reinforced electrically conductive aromatic polydisulfide/expanded graphite nanocomposites, Mater. Chem. Phys. 93 (2005) 122-128.

[16] B. Yao, G. Wang, J. Ye, X. Li, Corrosion inhibition of carbon steel by polyaniline nanofibers, Mater. Lett. 62 (2008) 1775-1778.

[17] S.A. Gordeyev, J.A. Ferreira, C.A. Bernardo, I.M. Ward, A promising conductive material: highly oriented polypropylene filled with short vapour-grown carbon fibres, Mater. Lett. 51 (2001) 32.

[18] E. Hablot, R. Matadi, S. Ahzi, L. Averous, Renewable biocomposites of dimer fatty acid-based polyamides with cellulose fibres: Thermal, physical and mechanical properties, Compos. Sci. Technol. 70 (2010) 504-509.

[19] S.Y. Fu, B. Lauke, E. Mader, X. Hu, C.Y. Yue, Fracture resistance of short-glass-fiber-reinforced and short-carbon-fiber-reinforced polypropylene under Charpy impact load and its dependence on processing. Journal of Materials Processing Technology 89-90 (1999) 501-507.

[20] S.Y. Fu, B. Lauke, E. Mader, C.Y. Yue, X. Hu, Tensile properties of short-glass-fiber and short-carbon-fiber-reinforced polypropylene composites. Composites: Part A 31 (2000) 1117-1125.

[21] S. Ramakrishna, F. Kazutoshi, T. Wee-Eong, L. Teik-Cheng, M. Zuwei, An introcduction to electrospinning and nanofibers, World Scientific Publishing Co. Pte. Ltd. (2005) 7-21.

[22] S.N. Amrinder, C.W. Joanna, A. Cristina, S. Metin, Drawing suspended polymer micro-/nanofibers using glass micropipettes, Appl. Phys. Lett. 89 (2006) 183105-18308.

[23] X. Xiaobo, W. Yuqing, L. Baojun, Nanofiber drawing and nanodevice assembly in poly (trimethylene terephthalate), Optics express, 16 (2008) 10815-10822.

[24] F. Lin, L. Shuhong, L. Huanjun, Z. Jin, S. Yanlin, J. Lei, Z. Daoben, Super-hydrophobic surface of aligned polyacrilonitrile nanofibers, Angew Chem. Int. Ed. 41 (2002) 1221-1223.

[25] T.G James, T. Hashimoto, K. Saijo, Polystyrene-block-poly(2-cinnamoylethyl methacrylate) nanofibers preparation, characterization, and liquid crystalline properties, Chem. Eur. J. 5 (1999) 2740-2749.

[26] G. Liu, L. Qiao, A. Guo, Diblock copolymer nanofibers, Macromolecules 29 (1996) 5508-5510.

[27] K. de Moel, G. O. R. A. Ekenstein, H. Nijland, E. Polushkin, G. ten Brinke, Polymeric Nanofibers prepared from self-organized supramolecules, Chem. Mater. 13 (2001) 4580 – 4583.

[28] M.M. Munir, A.B. Suryamas, F. Iskandar, K. Okuyama, Scaling law on particle-to-fiber formation during electrospinning, Polymer 50 (2009) 4935–4943.

[29] S.L. Shenoy, W. D. Bates, H.L. Frisch, G.E. Wnek, Role of chain entanglements on fiber formation during electrospinning of polymer solutions: good solvent, non-specific polymer–polymer interaction limit, Polymer 46 (2005) 3372–3384.

[30] D. Li, Y. Xia, Direct fabrication of composite and ceramic hollow nanofibers by electrospinning, Nano Lett. 4 (2004) 933–938.

[31] X. Li, Q. Qian, W. Zheng, W. Wei, X. Liu, L. Xiao, Q. Chen, Y. Chen, F. Wang, Preparation and characteristics of LaOCl nanotubes by coaxial electrospinning, Mater. Lett. 80, (2012) 43-45.

[32] D. Han, A.J. Steckl, Superhydrophobic and oleophobic fibers by coaxial electrospinning, Langmuir 25 (2009) 9454–9462.

[33] A.L.Yarin, Coaxial electrospinning and emulsion electrospinning of core–shell fibers, Polym. Adv. Technol. (2011) 22 310–317.

[34] L.D. Tijing, A. Amarjargal, Z. Jiang, M.T.G. Ruelo, C.H. Park, H.R. Pant, D.W. Kim, D.H. Lee, C.S. Kim, Antibacterial tourmaline nanoparticles/polyurethane hybrid mat decorated with silver nanoparticles prepared by electrospinning and UV photoreduction, Curr. Appl. Phys. 13 (2013) 205-210.

[35] N.A.M. Barakat, M.F. Abadir, F.A. Sheikh, M.A. Kanjwal, S. J. Park, H.Y. Kim, Polymeric nanofibers containing solid nanoparticles prepared by electrospinning and their applications, Chem. Eng. 156 (2010) 487-495.

[36] D.P. Macwan, P.N. Dave, S. Chaturvedi, A review on nano-TiO_2 sol–gel type syntheses and its applications, J. Mater. Sci. 46 (2011) 3669–3686.

Chapter 2

One-step fabrication of short electrospun polymer fiber by electric spark

2.1. Introduction

The short fiber fabrication process has been drawn a tremendous attention of many researchers due to the broad applications of short fibers, which varied from mechanical engineering to corrosion protection. Short fibers were applied as filler or reinforcement to improve the electrochemical, thermal properties, and mechanical of polymer matrix. Fu et. al reported that short carbon fibers and short glass fibers reinforced to the polymer matrix have enhanced the tensile properties [1,2]. This composite is applicable for aerospace and automotive industries, due to its lightweight and excellent mechanical properties. In corrosion protection field, adding the polyanilinne (PANI) short fibers into the coating process of carbon steel (CS) has enhanced the corrosion resistance of coated carbon steel [3]. The thermomechanical stability of poly (butylene succianate) has greatly improved by introducing biodegradable reinforcement of short silk fiber [4]. This performance improvement of an environmentally friendly material makes biocomposites industrially applicable.

Recently, the process of short fibers fabrication usually involved the mechanical, thermal, and polymerization processes. These processes are responsible for the formation of the short fibers. Each process has yielded short fibers that range in size from millimeters to nanometers and each has several drawbacks. Yao et al. [3] has used Interfacial polymerization to fabricate PANI short fibers ranging from 200-400 nm. The monomers of aniline were dissolved in chloroform then the interfacial

polymerization was conducting in a mixture of HCl and ammonium persulfate solution. This process is expensive and environmentally harmful due to the use of an acid chloride reactant and a toxic solvent. Fu et al. [1] have been employed Extrusion compounding and injection molding processes in order to fabricate short-glass-fiber and short-carbon-fiber reinforcement with length ranging from 150-300 μm. The glass and carbon roving fibers were melted at 214-239 ^{o}C using a twin-screw extruder then the cooled extruded strands were chopped mechanically to form short fibers. In order to form a composite polymer bulk, these short fibers were injection-molded with polypropylene at 210-230 ^{o}C forming a dumbbell-shaped composite. The high temperature and many-staged processes reduce the cost-effectiveness of this method. These problems have encouraged many researchers to seek effective process for the fabrication of short fibers.

The effective method to fabricate short fiber have been performed and developed. The research has focused on electrospinning-based fabrication due to its wide application, and due to the simple process and efficient for the fabrication of polymer composite nanofibers [5] and ceramic nanofibers [6]. The electrospinning technique utilizes a high voltage, which applied to a viscous polymer solution in order to create an electrified jet. The surface charges were generated on the solution and then it continuously stretched by electrostatic repulsions between the surface charges and the evaporation solvents, forming polymer fibers [5]. Generally, electrospinning technique fabricates continuous fibers therefore cutting process is necessary to obtain short fibers. A photocross-linking under influence of UV-radiation has been employed as a cutting method by Stoiljkovic and Agarwal [7] in order to produce 20-150 μm short fibers. They employed the concept of a polymer chain photocross-linking reaction upon UV

radiation. The solution precursor for electrospinning was double-bound polymers solution including a photocross-linker and a photoinitiator. The obtained electrospun fibers were irradiated by UV in the presence of a mask slit. The uncovered electrospun fibers were cross-linked and insoluble, whereas the covered fibers were non-cross-linked and soluble in the appropriate solvent. The short fibers were obtained by immersing the irradiated fibers into the appropriate solvent. However, the length of the fibers was limited by the width of the mask, and the process took more than one-step. Yoshikawa et al. [8] reported the fabrication of shortened electrospun polymer fibers with a well-defined concentrated polymer brush. This method was dividing into three major processes, which are electrospinning of continuous fiber, brush-like formation, and mechanical cutting. The first process was electrospinning of polymer solution to fabricate continuous fiber. The second process was the brush formation on the surface of continuous electrospun fibers using atom transfer radical polymerization method. The last process was the cutting process of these continuous fibers in the water using homogenizer for 1 to 3h. The short fibers were 11μm in length and controllable by adjusting the cutting time in the water. However, this technique requires several steps and much time for the polymerization and cutting of the fibers. The current cutting methods are not entirely convenient and require a relatively long amount of time due to the secondary process; therefore, a simple and straightforward cutting method is necessary.

The cutting technique via an electric spark established in electrical discharge machining (EDM) can be applied to the fabrication of short fibers. EDM is well-known method to cutting and material machining process via an electric spark. This method is a machining process for the manufacturing of geometrically complex and hard material

parts. The thermal energy of the electric spark initializes a substantial amount of heating and melts the material on the surface of solid metal [9]. The electric spark can be simply generated between the tips of two electrodes by applying a high voltage to one of them and by keeping the other one at ground level. The occurrence of electric spark is dependent on the amplitude of the electric field and on the distance between the tips of the two electrodes [10].

In this Chapter, a one-step process for the production of short polymer fibers using an electrospinning technique and periodic electric spark was proposed. Different from the current electrospinning-based techniques, the cutting process was conducted in situ by electric spark during electrospinning of polymer precursor. A single step and relatively simple and low cost process could be achieved using this method. The electric spark was generated by adjusting the distance between the tips of two electrodes, then applying a voltage to the electrodes. A biodegradable polymer of cellulose acetate was employed. A solution of cellulose acetate and organic solvent was ejected from a syringe needle and was stretched by the electric field then it cut after passed through the gap between the tips of two electrodes that generated an electric spark with frequency of 5 kHz. The lengths and diameters of the obtained short electrospun polymer fibers are characterized herein, as well as the cutting mechanism used to obtain the short electrospun polymer fibers.

2.2. Experimental methods

2.2.1. Preparation of polymer solution

Cellulose acetate (CA, Sigma Aldrich, UK) with a molecular weight (Mw) of 30,000 was used. The solvent was a mixture of acetone (99.5% of purity, Kanto

Chemical, Japan) and N,N-dimethyl formamide (DMF) (99.5% of purity, Wako Chemical, Japan) at a volume ratio of 2:1. DMF was mixed with acetone in order to delay the evaporation of acetone during electrospinning [11]. The total volume fraction of CA in the solution was set at 13 vol %. The polymer solution for electrospinning was prepared by pouring the CA powder into a glass bottle containing solvent. The mixture of CA and solvent in the closed bottle was then stirred using a magnetic stirrer for several hours until a homogenous solution was obtained (**Figure 2.1**).

Figure 2.1. Precursor solution of cellulose acetate.

2.2.2. Experimental setup

A schematic of the apparatus and an actual photograph used to electrospin and cut the polymer fibers is shown in **Figures 2.2a** and **b**, respectively. The apparatus consisted of a micro syringe pump (ESP64, EiCom Corporation), a 1,000 cc syringe (TTL 2-432, Hamilton Company) with a stainless needle (OD: 0.8 mm, ID: 0.5 mm),

two aluminum rods 1.6 mm in diameter with sharp ends that were used as electrodes to generate an electric spark, a collector plate of aluminum foil (30 x 30 mm), three high-voltage power supplies (HV1, 0-HER-15P5-LV, Matsusada Precision Inc.; HV2,HERR-15P5-LG, Matsusada Precision Inc.; HV3, PHS 35K-3, Kikusui Electronics Corporation), and a function generator (Wave Factory 1945, NF Corporation). The polymer solution was transferred to the syringe at a flow rate of 0.5 μL/min, and it was ejected from the needle tip, which was connected to the HV1. The flowing polymer was adhered onto the collector plate, which was connected to the HV2. The distance between the needle tip and the collector plate was set to 32 mm. Two electrodes were used to generate an electric spark and were set at a distance of 12 mm from the needle. The distance between the tips of the electrodes was set to 1.5 mm; one electrode was connected to the HV3 and a function generator, and the other one was connected to the ground. Humidity and temperature were maintained at 60% and 20 ºC via a humidifier and a temperature controller (PAU-300S, Apiste Corporation).

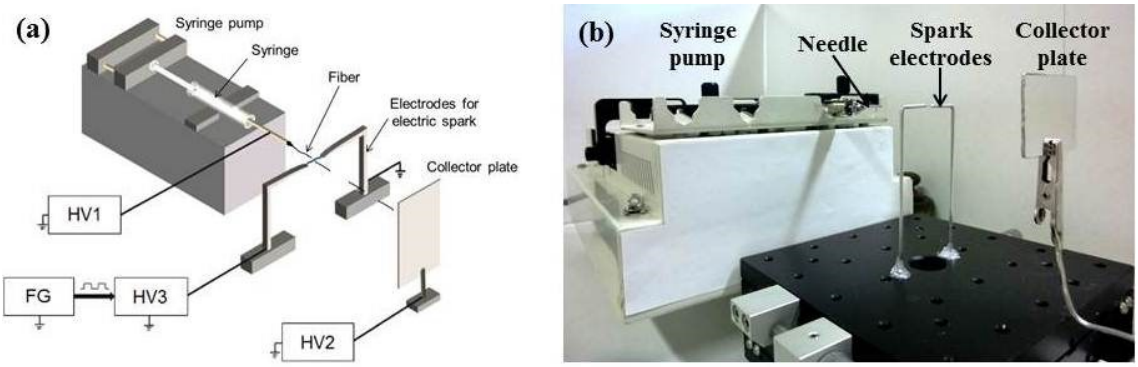

Figure 2.2. Schematic of instrument set-up employed for one-step fabrication of short electrospun fibers using electric spark: (a) Illustration Image; (b) actual photograph.

2.2.3. Observation of electric spark and frequency measurement

The generation of an electric spark by the tips of the two electrodes was observed using a CCD camera with a resolution of 0.4 MP, twice-digital zoom, and 0.8 lux of minimum illumination (MTV-73x11HN, Mintron Enterprise Co., Ltd). A monocular optical lens with a diameter of 50 mm and a magnification factor of 8 (M0850, Specwell) was attached to the CCD camera. The images were taken at a speed of 30 fps and were recorded on a personal computer (PC). The condition of the electric spark when a polymer solution was flowed between the tips of the two electrodes was also observed. The CCD camera was placed above the two electrodes to capture the electric spark. The PC recorded these conditions for 2 min, and still images were cut from the video that was produced.

The frequency of the electric spark was analyzed from a beat sound that occurred during the electric spark. When the electric spark occurred, an electric current transient went through the spark channel and produced an intense release of heat. This rapid thermal change caused a sharp rise in pressure, which generated a beat sound due to the sonic waves [12]. The sound was recorded as a waveform on the PC through audio analyzer software (Audacity 1.3 Beta) and a microphone for 50 s with a sampling rate of 44 ksps. The waveform was plotted and analyzed in the time domain using the same audio analyzer software to find peaks showing the beat sounds. The peaks images in different time resolutions (**Figures 2.4** and **2.5**) were printed on the screen, then the time interval between the peaks were measured by image processing software (Ruler ver. 0.002) to obtain the frequency of the electric spark. During the spark measurement, the values for temperature and humidity were maintained under the same conditions as those of electrospinning.

2.2.4. Short electrospun polymer fiber observation

The prepared short fibers were observed by SEM (JSM-6340F, JEOL Ltd.) with a maximum magnification factor of 650,000x and a resolution of 1.2 nm at an acceleration voltage of 20 kV. The shape of the short fibers was evaluated by measuring the diameter at the centers and the edges of the fibers, which were also compared with those of the continuous electrospun polymer fibers.

The distribution of the lengths of the short electrospun polymer fibers was measured using the ruler function of image processing software during observation using a digital microscope with a resolution of 2.11 MP (VH-8000, Keyence Corporation) and a high-range zoom lens with a magnification ranging from 450 - 3,000x (VH-Z450, Keyence Corporation). The distribution of the diameters of the center parts of the short fibers was noted. The mean length and diameter of the short fibers was calculated from the measurement of approximately 200 fibers.

2.3. Results and discussion

2.3.1. Condition of electric spark

Figure 2.3 shows the typical electric spark generated within a spark gap. A bluish-white electric spark was observed with a center diameter of approximately 0.5 mm. To generate electric spark, sufficient voltage was generated within the spark gap. In this experiment, the electrodes had sharp ends and the breakdown voltage of the electric spark was found at 3.5 kV with a spark gap of 1.5 mm. Compared to the spherical electrodes, the electrodes with sharp ends gave a lower voltage breakdown for the generation of electric spark [12]. Due to the distance ratio of the spark gap and the

needle-collector (1:21), the electric field generated between the needle and the collector was found to have not significantly affected the electric spark.

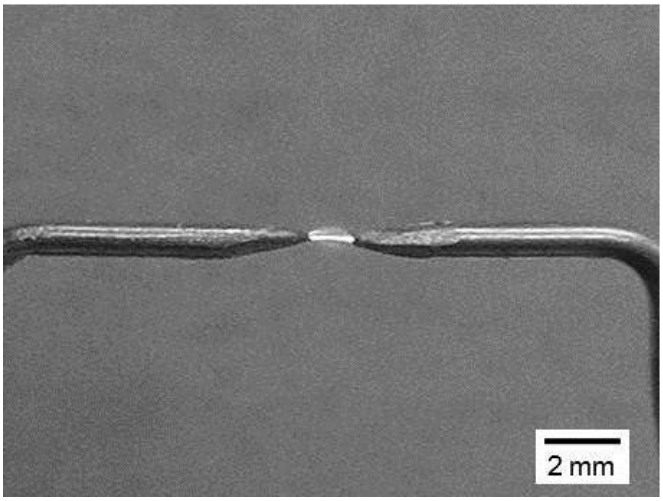

Figure 2.3. Condition of the typical electric spark occurred between the tips of two electrodes. Electric spark was observed with a center diameter of approximately 0.5 mm.

The characteristics of an electric spark were investigated by detecting and recording the sound waves produced by an electric spark. Two voltages, 3.6 and 4.1 kV, were applied to investigate the characteristics of a typical sound wave. **Figures 2.4a** and **b** show a typical sound wave over a 1 sec period generated at both voltages, respectively. There were 18 and 33 spikes at voltages of 3.6 and 4.1 kV, respectively. As the time resolution for **Figures 2.4a** and **b** was increased, each spike at both voltages was recognized as damped oscillation with a frequency of 5 kHz (**Figure 2.5**). These results confirm that the typical sound wave of an electrical spark has a damped oscillation with a repetitive occurrence. The occurrence interval of a damped oscillation was more uniform at 4.1 kV than it was at 3.6 kV. Due to the occurrence interval of the damped oscillation, the electric spark generated at 4.1 kV was reliable for the fabrication of short fibers.

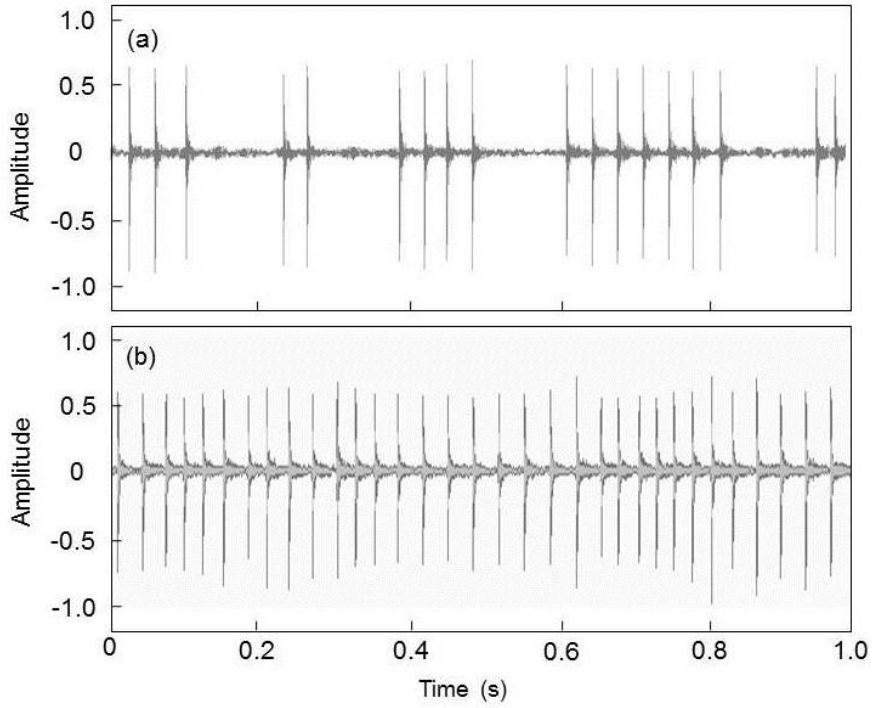

Figure 2.4. The typical sound wave generated by an electric spark at: (a) 3.6 kV; (b) 4.1 kV

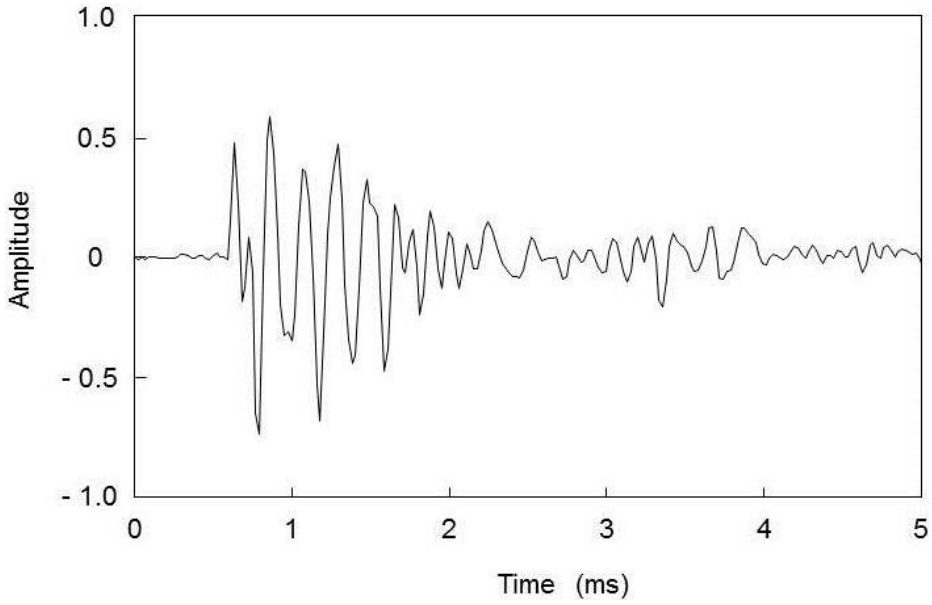

Figure 2.5. The typical sound wave of electric spark is recognized as damped oscillation with frequency of 5 kHz. Observation is obtained from typical sound wave at 4.1 kV by increasing the time resolution.

2.3.2. Preparation of short electrospun polymer fiber

The short fibers were prepared by electrospinning that included an electric spark to cut the fibers. A polymer solution was ejected from a syringe into the collector and partially through the electric spark gap. The fibers that flowed through to the electric spark gap were cut and short fibers were found on the collector plate with a density of 1-5 fibers per 0.12x0.2 mm^2, whereas the fibers that did not flow through to the electric spark were uncut and remained as continuous fibers on the collector plate. The continuous fibers were dominant on the collector plate due to the limited size of the cutting area of the electric spark: 1.5x0.5 mm^2 (**Figure 2.3**). For comparison, the continuous fibers were also prepared by a common electrospinning set up. A comparison of the diameters of short fibers and continuous fibers was performed to study the influence of electric spark on fiber fabrication.

Figure 2.6 shows the SEM images of prepared short fiber and continuous fibers produced by the method outlined in this chapter and by common electrospinning, respectively. The length of the short fiber was approximately 100 μm, and one edge was curled (**Figure 2.6a**). The rectangle boxes in **Figure 2.6a** are magnifications of the center and the edge parts of the short fiber that show the diversity in diameter. The diameters at the center part ranged from 500 to 1000 nm (**Figure 2.6b**). The edge of the short fiber was not smooth (**Figure 2.6c**), and the diameters varied from 200 to 140 nm, which was narrower than that of the center part of the short fiber. From the observation of the shape of the short fiber, it seems apparent that the electrospun fiber was stretched and cut by the periodic electrical field and thermal energy from the electric spark, respectively.

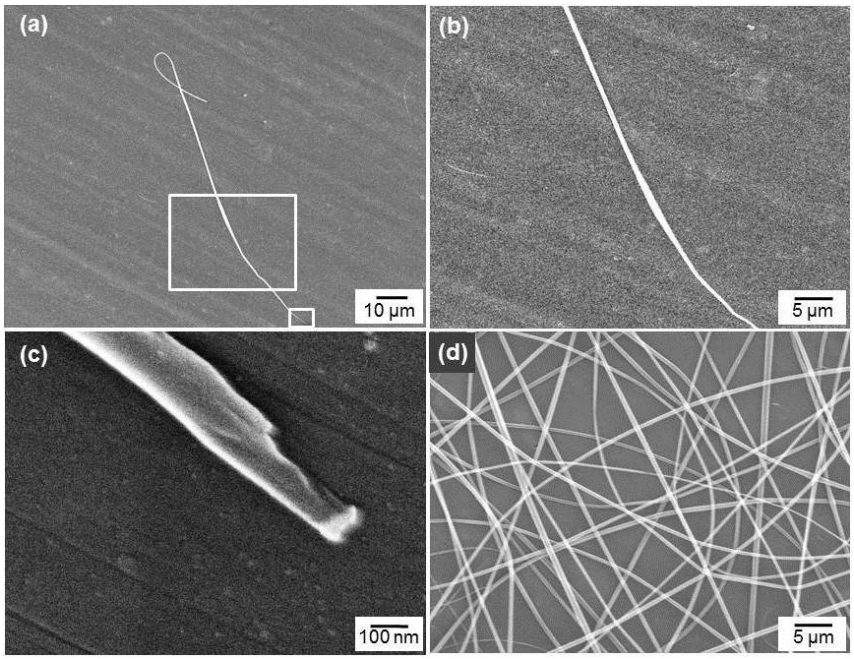

Figure 2.6. SEM images of (a) a short fiber, (b) the center of a short fiber, (c) the edge of a short fiber, and (d) a continuous electrospun fiber without an electric spark.

The diameters of continuous electrospun fibers produced by common electrospinning (**Figure 2.6d**) varied from 90 to 400 nm. Compared with the diameters of the short fibers, the diameters at the edges of the short fibers were smaller than those of the continuous fibers, and the diameters at the centers of the short fibers were larger than those of the continuous fibers. This indicated that the short electrospun fibers were not only stretched but were also compressed. The electric field generated by the electric spark blocked the fiber flow, so that it compressed the mass in the centers of the short fibers.

Figure 2.7 shows the distribution of the lengths of the short electrospun fibers, which were measured by optical microscope. The lengths varied from 22 to 1,000 μm. Most of the short fibers prepared in the experiment ranged from 22 to 400 μm in length, although a small amount of the fibers had lengths ranging from 500 to 1,000 μm. This result confirmed that short fibers were fabricated although the continuous fiber was still

observed. The mean length of the short fibers was 230 μm. **Figure 2.8** shows the distribution of the diameters for the centers of the short fibers. The diameters primarily ranged from 0.6 to 1.4 μm. The mean diameter of the short fibers was 1 μm.

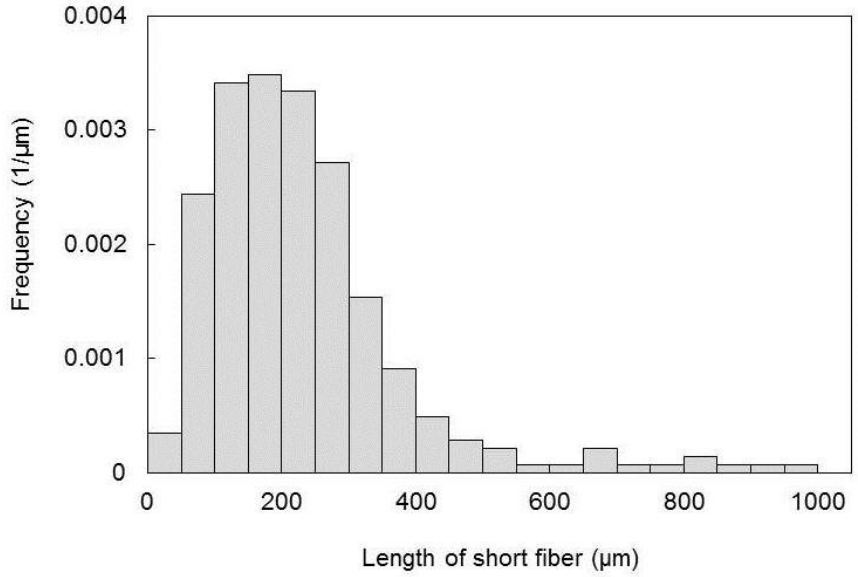

Figure 2.7. The distribution of the lengths of the short fibers.

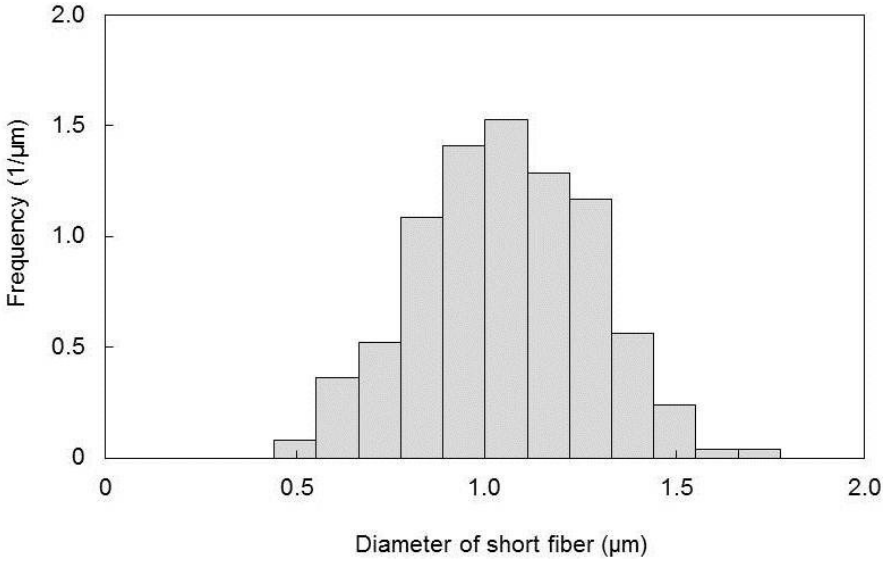

Figure 2.8. The distribution of the diameters of the short fibers.

2.3.3. Cutting mechanism of short electrospun polymer fiber

In order to confirm the mechanism of fiber cutting, the video and images around the electric spark gap were captured and recorded on a PC. The fiber motion in electrospinning was random, however, in this experiment the fibers had passed the spark gap and the image was captured successfully. As the polymer solution was ejected, the spark cut the fiber. Truncated fibers were on the left and the right sides of the electric spark (**Figure 2.9a**). As the electric spark cut the fiber, it had a wide shape with a bluish-white color in the center and a red color on the left and the right sides. For comparison, the condition of the electric spark without a polymer solution ejected from the needle was obtained (**Figure 2.9b**). The electric spark had a straight and slim shape with a bluish-white color. These results confirmed that fiber flowed toward the spark gap then the electric spark burned and truncated it in one particular spot.

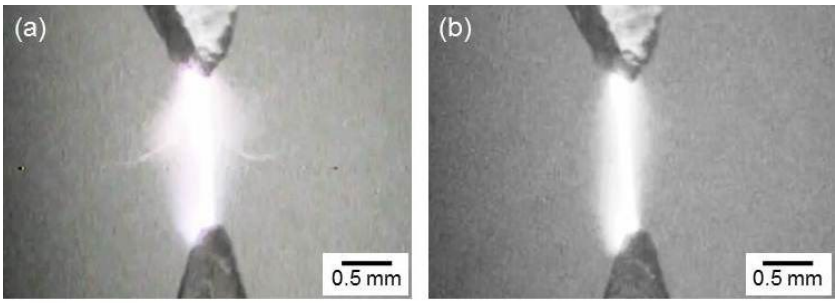

Figure 2.9. The conditions of electric sparks: (a) the electric spark was cutting the fiber as the polymer solution was ejected; (b) the polymer solution was not ejected.

For further analysis, the temperature distribution of the steady-state condition around an electrical spark was also estimated. Based on the temperature distribution, the cutting points were estimated. The temperature distribution along the x-y axis was derived as follows:

$$\frac{\partial}{\partial x}\left(\lambda_x \frac{\partial T}{\partial x}\right)+\frac{\partial}{\partial y}\left(\lambda_y \frac{\partial T}{\partial y}\right)=-q-c\rho\frac{\partial T}{\partial t} \quad (1)$$

Eq. (1) can be solved numerically using a 2D finite element method (Quickfield, Tera Analysis Ltd.), where λ_x and λ_y are components of the heat conductivity tensor on the x-y axis [W/K.m], T is the temperature [K], q is the volume power of the heat source [W/m^3], c is the specific heat of air [J/kg.K], and ρ is the density of air [kg/m^3]. The initial ambient temperature is set at 293 K and the melting point of cellulose acetate is 533 K (Material Safety Data Sheet). Electric spark power was calculated from the data of voltage applied and the electric current (V=4.1 kV**,** I=0.8 mA). It was assumed that electric spark has a cylindrical shape with a cross-sectional diameter and height that are 0.5 mm and 1.5 mm, respectively. The volume power of the heat source was obtained by dividing the electric spark power by the volume of the electric spark to yield 1.1x10^{10} W/m^3. For analysis simplicity, the volume power of the heat source was assumed to be constant over the time. **Figure 2.10** shows the temperature distribution for a 1 mm radius with respect to the center of the electric spark. The results confirmed that cutting points lie in a radial direction from the center of a spark up to 0.22 mm (shaded area in **Figure 2.10**). These results also confirmed that high temperatures of an electric spark are distributed within the electric spark in a radius of less than 0.5 mm. This result agreed with that found by Zeng and Zhao [13].

With regard to the cutting of an electrospun fiber by an electric spark, the length of a short electrospun fiber should be related to the linear velocity of the polymer solution and to the frequency of the electric sparks. We considered that only the fibers with linear motion were cut by an electric spark, therefore the calculation could be

simplified. The linear velocity of the polymer solution from the needle tip to the collector plate can be calculated using the following equation:

$$v = Q/A \quad (2)$$

where v, Q, and A are the linear velocity of the precursor solution [m/s], the flow rate of the polymer solution [m^3/s], and the cross-sectional area of the flowing polymer solution [m^2], respectively. The flow rate of the precursor solution was 8.3×10^{-12} m^3/s (= 0.5 μL/min). When the precursor solution ejected from the needle tip formed a fiber in air, the solvent was evaporated leaving only the polymer on the fiber. The cross-sectional area of a flowing polymer solution of 7.9×10^{-12} m^2 (= $\pi \times 0.5^2$ / 0.13 μm^2) was calculated based on a prepared short fiber with a diameter of 1 μm and a polymer concentration of 13 vol. %. As a result, the linear velocity of the polymer solution was calculated to be 1.05 m/s. This agreed with the experimental results found by Reneker et al. [14].

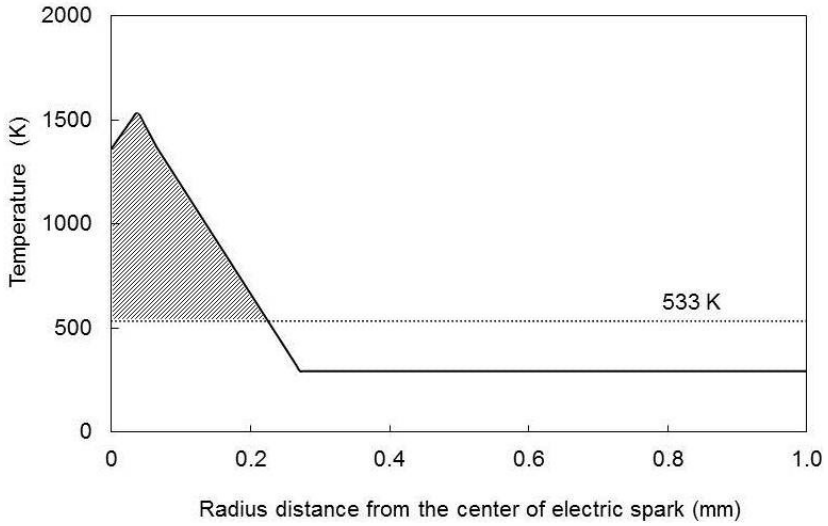

Figure 2.10. The temperature distribution for the center portion of the electric spark. The melting temperature of cellulose acetate is 533 K and cutting points are marked by the shaded areas from the center of the electric spark and extending for 0.22 mm.

The length of the short electrospun fiber was predicted by dividing the linear velocity of the polymer solution by the frequency of the damped oscillation of the electric spark, as follows:

$$l = v/f = Q/Af \quad (3)$$

where l and f are the length of the short electrospun fiber [m] and the frequency of the electric spark [Hz], respectively. The fiber length calculated from 5 kHz was 271 μm. This calculation approximated the measured fiber length of 230 μm, thus confirming that the cutting to prepare a short fiber was due to an electric spark of 5 kHz. The dispersion of the distribution of the lengths of the short fibers shown in **Figure 2.7** was caused by a fluctuation in the flow rate of the polymer solution, by different cutting points, and by the dumped oscillation of an electric spark. There were 5-7 peaks in the damped oscillation of 5 kHz with decaying amplitude, as shown in **Figure 2.5**. We suspected that some peaks did not cut the fibers, so that short fibers with lengths of 400-1,000 μm were created. We suspected that the variation of the cutting point in a radial direction also affected the distribution of the lengths of prepared short fibers.

In order to control the lengths of the short fibers, it was useful to control the flow rate of the polymer solution, the frequency of the electric spark, and the trajectory of fibers. Some improvements in this method are required in order to enhance the efficiency of the production of short fibers. This method of using an electric spark for cutting will be very useful for applications in industrial production, because of the one-step fabrication.

2.4. Conclusions

The one-step fabrication process of short electrospun fibers was successfully developed. The one-step fabrication process was combining an electrospinning method and electric spark generation at once time. High voltage with a square wave was applied to two electrodes to generate a periodic electric spark that could be recognized at 4.1 kV. As a solution of cellulose acetate and organic solvent was ejected from a syringe needle and was stretched by the electric field then it cut after passed through the gap between the tips of two electrodes that generated an electric spark with frequency of 5 kHz. The short fibers of average 231 μm were found on the collector plate with a density of 1-5 fibers per 0.12x0.2 mm2, whereas the fibers that did not flow through to the electric spark were uncut and remained as continuous fibers on the collector plate. The theoretical fiber length was calculated at 271 μm when employing a 5 kHz of electric spark, which was in good agreement with the length of the short fibers obtained in the experiment.

2.5. References

[1] S.Y. Fu, B. Lauke, E. Mader, X. Hu, C.Y. Yue, Fracture resistance of short-glass-fiber-reinforced and short-carbon-fiber-reinforced polypropylene under Charpy impact load and its dependence on processing, J. Mater. Process. Technol. 89-90 (1999) 501-507.

[2] S.Y. Fu, B. Lauke, E. Mader, C.Y. Yue, X. Hu, Tensile properties of short-glass-fiber and short-carbon-fiber-reinforced polypropylene composites, Compos. : Part A 31 (2000) 1117-1125.

[3] B. Yao, G. Wang, J. Ye, X. Li, Corrosion inhibition of carbon steel by polyaniline nanofibers, Mater. Lett. 62 (2008) 1775-1778.

[4] S.M. Lee, D. Chao, W.H. Park, S.G. Lee, S.O. Han, L.T. Drzal, Novel silk/poly(butylene succinate) biocomposites: The effect of short fibre content on their mechanical and thermal properties, Compos. Sci. Technol. 65 (2005) 647-657.

[5] D. Li, Y. Xia, Electrospinning of nanofibers: Reinventing the wheel, Adv. Mater. 16 (2004) 1151-1170.

[6] H. Wu, W. Pan, , D. Lin, H. Li, Electrospinning of ceramic nanofibers: Fabrication, assembly and application, J. Adv. Ceramics 1 (2012) 2-23.

[7] A. Stoiljkovic, S. Agarwal, Short electrospun fibers by UV cutting method, Macromol. Mater. Eng. 293 (2008) 895-899.

[8] C.Yoshikawa, K. Zhang, E. Zawadzak, H. Kobayashi, A novel shortened electrospun nanofiber modified with a ‘concentrated’ polymer brush, Sci. Technol. Adv. Mater. 12 (2011) 1-7.

[9] K.H. Ho, S.T. Newman, State of the art electrical discharge machining, Int. J. Machine Tools Manufacture 43 (2003) 1287-1300.

[10] J.J. Lowke, Theory of electrical breakdown in air: the role of metastable oxygen molecules, J. Phys. D: Appl. Phys. 25 (1992) 202-210.

[11] Z. Ma, M. Kotaki, S. Ramakrishna, Electrospun cellulose nanofiber as affinity membrane, J. Membrane Sci. 265 (2005) 115-123.

[12] E. Martinson, J. Delsing, Electric spark discharge as an ultrasonic generator in flow measurement situations, Flow Measurement and Instrumentation 21 (2010) 394-401.

[13] H. Zeng, Y. Zhao, Microfabrication in electrospun nanofibers by electrical discharges, Sensors and Actuators A: Physical 166 (2011) 214-218.

[14] D.H. Reneker, A.L. Yarin, H. Fong, S. Koombhongse, Bending instability of electrically charged liquid jets of polymer solutions in electrospinning. J. of Appl. Phys. 87 (2000) 4531-4547.

Chapter 3

A simple one-step fabrication of short polymer nanofibers via electrospinning

3.1. Introduction

Recently, short fiber has attracted tremendous attention of researcher due to the good performance as filler in the composite material. The short fiber filler has ability to enhance the tensile strength, conductivity, corrosion resistance, and thermal stability of polymer composites, which make it applicable in many fields such as in the aerospace industry, in the automotive industry, for corrosion protection, in flexible displays, as electrodes, etc. [1-8]. The diameter and length control of short fibers are the important factors in enhancing the properties of a polymer composite [9-12]. The general method for the preparation of controllable length and diameter of short fibers is a vapor-grown technique [13-15]. In this technique, the length and diameter of short fibers can be controlled by altering the catalyst size, temperature processing, and catalyst activity [13,14]. This technique is widely used in industry; however, several drawbacks are persisting such as an extended chemical route and post-processing, which necessary in order to enhance the physical properties of the carbon fibers. Due to this problems, the researchers have made various efforts to find more effective methods for the fabrication of short fibers [16,17].

The simplest and most reliable technique to fabricate polymer fiber with diameter varied from micro to nanometer is electrospinning. This technique utilizes a high voltage in order to electrified viscous polymer solution. The surface charges are generated on the drop of polymer solution then the Taylor cone shape is forming due to

the rapid increase of surface charges. The Taylor cone is continuously stretched into a jet by electrostatic repulsions between the surface charges and the evaporation solvents, forming continuous polymer fibers [18]. The important factors in the electrospinning technique are properties of precursor solution such as conductivity and dielectric constant of solvent, chain entanglement of polymer, viscosity, and surface tension. These properties are affected by solvent selection, polymer solution concentration and solubility of the polymer in the solvent, which allowed the transition from electrospraying to electrospinning. Luo et al has been demonstrated the spinnability-solubility maps for the polymethylsilsesquioxane (PMSQ) and poly(ε-caprolactone) (PCL) based on solvent selection and polymer solubility. However, electrospinning technique can only produces continuous fibers. In order to fabricate short fibers from the continuous electrospun fibers, secondary processes are applied [16,17]. As stated in the introduction of Chapter 1, Stoiljkovic et al. [16] and Yoshikawa et al. employed the secondary process in order to fabricate short polymer fiber from continuous electrospun fibers. The concept of Stoiljkovic et al. is a photocross-linking reaction under UV radiation as a secondary process [16], while the Yoshikawa et al. using a mechanical crushing by homogenizer as a secondary process [17]. Although the length of fiber can be controlled by these methods, the many stages processes were caused this method not effective.

The one-step process of short micro-fibers fabrication has been reported by Luo et al. The length of short micro-fibers could be changed by altering the molecular weight of PMSQ and using a volatile solvent, although the diameter of the short fibers is on a micro-order [21]. A low molecular weight of PMSQ resulted in shorter micro-fibers. However, a mechanism for the formation of short micro-fibers has not been

developed, and controlling the fiber length by altering polymer molecular weight could not be performed during the electrospinning process. The other method to fabricate discrete nanofiber is a pressurized gyration process, which resulted in nanofibers with length varied from 200 to 800 mm. the control of fiber length has been achieved by altering the rotational speed [23]. This method has the advantage of not requiring such high voltage and offers mass production capabilities, but the length of the nanofiber is too long for use as filler in the composite material. We have reported a one-step fabrication of short fibers using an electrical spark to cut the fibers during electrospinning in Chapter 1 [22]. The length of the short fibers is dependent on the frequency of the electrical spark; however, the range for the controlled length of the short fibers is narrow due to the difficulties with the frequency of the electrical spark.

In this chapter, a simple one-step fabrication of short polymer nanofibers by electrospinning was investigated. The effect of the concentration of the polymer solution, applied voltage, and the flow rate of the polymer solution on the fabrication of short nanofibers was investigated. The values for the length and diameter of the fabricated short polymer fibers were measured in order to correlate the spinning conditions. Herein, we note our observations on the shape of the short nanofibers and the condition of the ejected polymer solution, and we describe the fabrication mechanism: the rapid increase in repulsive force generated a lateral perturbation that made the polymer solution jet spread. The rapid increase in the repulsive force from surface charges combined longitudinal forces from the applied voltage split the solution jet and segmented the nanofibers.

3.2. Experimental methods

3.2.1. Preparation of polymer solution

Cellulose acetate (CA, Sigma Aldrich, UK) polymer with a number-average molecular weight of 30,000 was used as an electrospun polymer fiber. Acetone (>99.5%, Kanto Chemical, Japan) and N,N-dimethyl acetamide (DMAc) (>99.5%, Wako Chemical, Japan) was mixed at a volume ratio of 2:1 as a solvent, and CA polymer powder was added to 15 mL of solvent in a glass bottle. A DMAc was mixed in order to delay the evaporation of acetone during electrospinning [24,25]. The polymer solution of polymer and solvent mixed in the glass bottle were then stirred using a magnetic stirrer for several hours until a homogenous solution was obtained. The concentrations of polymer in the polymer solution varied from 9 to 18 wt. %.

3.2.2. Electrospinning of the polymer solution

A conventional electrospinning setup was used to fabricate the polymer fibers [26-28]. The polymer solution was loaded into a 1,000 cc syringe (TTL 2-432, Hamilton Company) with a stainless needle (OD: 0.46 mm, ID: 0.26 mm). A high-voltage power supply (HER-15P5-LV, Matsusada Precision Inc.) was connected to the stainless needle to electrify the polymer solution. The flow rate of polymer solution was controlled via a micro syringe pump (ESP64, EiCom Corporation). A 30 mm x 30 mm aluminum plate that was used to collect the fibers was connected to the ground, and a 3 mm x 3 mm silicon wafer was attached on it to observe the fibers. The distance between the needle tip and the aluminum plate was set at 90 mm. The ambient temperature and humidity were maintained at 20 ºC and 60% using a temperature controller and an integrated humidifier (PAU-300S, Apiste Corporation), respectively. The voltage for

electrospinning was varied from 0 to 12.0 kV, and the flow rate of the polymer solution was varied from 0.01 to 0.7 μL/min. The syringe was washed by acetone before each of the solution replacements.

3.2.3. Observation of electrospun fiber

The distribution of the diameters and the lengths of the short electrospun polymer fibers were measured using the ruler function of image processing software during observation with a digital microscope at a resolution of 2.11 megapixels (VH-8000, Keyence Corporation). Two types of lenses, a low-range lens and a high-range zoom lens with a magnification ranging from 25-3,000x (VH-Z450, Keyence Corporation), were used for the observation. The distribution and the average lengths of the electrospun fibers were determined for more than 200 fibers.

The shapes of the short nanofibers were observed using a SEM (JSM-6340F, JEOL Ltd.) with a maximum magnification factor of 650,000x and a resolution of 1.2 nm at an acceleration voltage of 20 kV. The diameters at the centers and the edges of the short nanofibers were measured to confirm the stretching of the fibers.

The operation of the polymer solution jet was observed using a CCD camera with a resolution of 0.4 megapixels, a two-fold digital zoom, and 0.8 lux with a minimum illumination (MTV-73x11HN, Mintron Enterprise Co., Ltd). A monocular optical lens with a diameter of 50 mm and a magnification factor of 8 (M0850, Specwell) was attached to the CCD camera. The images were taken at a speed of 30 fps and were recorded on a personal computer.

3.3. Results and discussion

3.3.1. Effect of the polymer concentration in the polymer solution

The electrospun fibers were fabricated from a polymer solution of various polymer concentrations, and the morphology of the fibers was observed. The voltage for electrospinning was set to 4.4 kV, and the flow rate of the polymer solution was kept at 0.3 μL/min. As a result, three types of fibers were recognized: beaded fibers, short fibers, and continuous fibers. **Figure 3.1** shows the typical fibers fabricated from a polymer solution with various polymer concentrations. The beaded fibers were fabricated at polymer concentrations that ranged from 9 to 12 wt. %. **Figure 3.1a** shows typical beaded fibers fabricated at a concentration of 9 wt. %, with a diameter of fibers and beads that was approximately 300 nm and 2 μm, respectively. The fabrication of beaded fibers has previously been reported, and the effect of the polymer concentrations and solvent type on the shape of the beaded fibers has been discussed [25, 29, 30]. Since the polymer concentration ranged from 13 to 15 wt. %, short fibers could be fabricated. Typical short fibers fabricated at a polymer concentration of 13 wt. % are shown in **Figure 3.1b**. Both straight and curled shapes were recognized in the short fibers fabricated under these conditions. The lengths of the short fibers ranged from 50 to 150 μm, and the average diameter was 1 μm. Continuous fibers were fabricated from concentrations that ranged from 16 to 18 wt. %. **Figure 3.1c** shows continuous fibers fabricated from a polymer solution with a concentration of 18 wt. %, and an average diameter of 3 μm. The morphology of the fiber transformed generally from that of beaded fibers to continuous fibers as the polymer concentration increased [19,31]. However, short nanofibers could be fabricated at a concentration of 13-15 wt. % during the transformation from beaded fibers to continuous fibers. This was due to the effect of

the selected solvents and polymer, acetone and DMAc as the solvent, and cellulose acetate as the polymer. Santi et al. have reported that a solution of cellulose acetate in a 2:1 volume ratio of acetone/DMAc has a low surface tension [25], and that the solvent-polymer interaction has an influence on the tensile strength of the polymer solution, which results in fibers that are readily segmented. Thus, the shape of the fibers fabricated by electrospinning was largely dependent on the concentration of the polymer in the solution. Short fibers could be fabricated from polymer solutions that were 13 to15 wt. %.

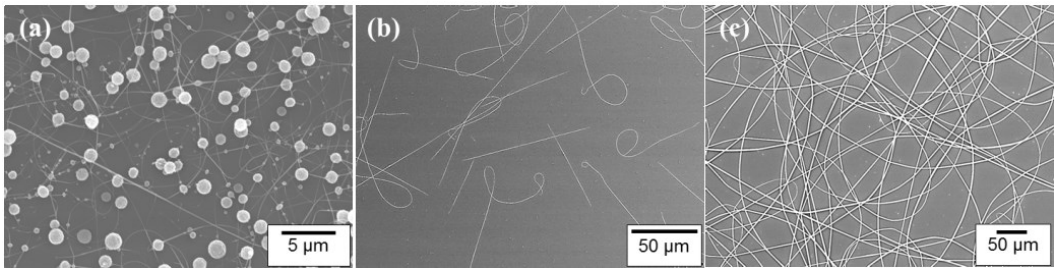

Figure 3.1. The electrospun fibers from a polymer solution with various concentrations: (a) 9 wt. %, (b) 13 wt. %, and (c) 18 wt. %. The voltage was 4.4 kV, and the flow rate of the polymer solution was 0.3 μL/min.

The diameter of the short fibers fabricated at a voltage of 4.4 kV and a flow rate of 0.3 μL/min (**Figure 3.1b**) was still large for nanomaterial applications, and resulted in a curled shape. In order to determine the optimal conditions to fabricate nano-sized and straight short fibers, further experiments were conducted. These experiments showed that short fibers with a nano-sized diameter and a straight shape could be fabricated by increasing the voltage and decreasing the flow rate of the polymer solution. **Figure 3.2** shows the optical micrographs of the short nanofibers fabricated from polymer solutions with concentrations of 13 to 15 wt. %. The voltage was 5.5 kV, and the flow rate was 0.1 μL/min. **Figure 3.3** shows the distribution of the diameters of short nanofibers that correspond with the short fibers shown in **Figure 3.2**. At a polymer

concentration of 13 wt. %, the average diameter of the short fibers was 320 nm with a narrow distribution (**Figure 3.3a**). As the polymer concentration increased to 14 and 15 wt. %, the diameter distribution increased to averages of 490 and 510 nm, respectively (**Figures 3.3bc**). **Figure 3.4** shows the distributions of the lengths of the short fiber that correspond to the short fibers shown in **Figure 3.2**. The short fibers fabricated from a polymer solution of 13 wt. % had an average length of 130 μm with a narrow distribution (**Figure 3.4a**). As the polymer concentration increased to 14 and 15 wt. %, the average length increased to 180 and 230 μm, and the distribution was broad (**Figures 3.4bc**). **Figure 3.5** shows the average lengths of short nanofibers fabricated at various polymer concentrations, and shows the morphologies. The error bars represent the standard deviation of the measured data. The average length of short nanofibers increased in a linear fashion with the polymer concentration, and could double with an increase in concentration of only 2 wt. %. Since more concentrated polymer solutions had a denser polymer chain entanglement, the polymer solution jet would stretch longer before breaking.

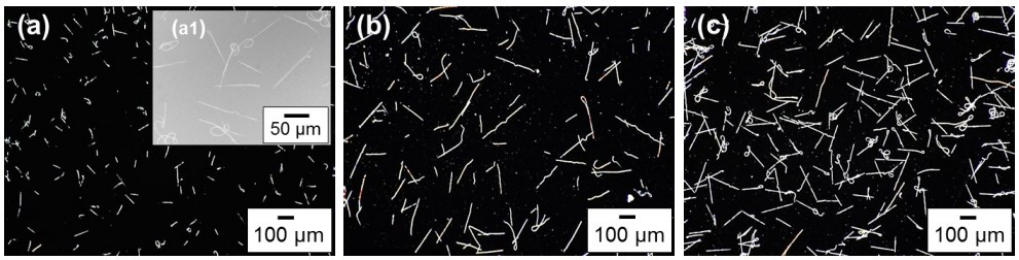

Figure 3.2. Optical micrograph of short fibers fabricated from polymer solutions with various concentrations: (a) 13 wt. %, (b) 14 wt. %, and (c) 15 wt. %. The voltage was 5.5 kV, and the flow rate was 0.1 μL/min.

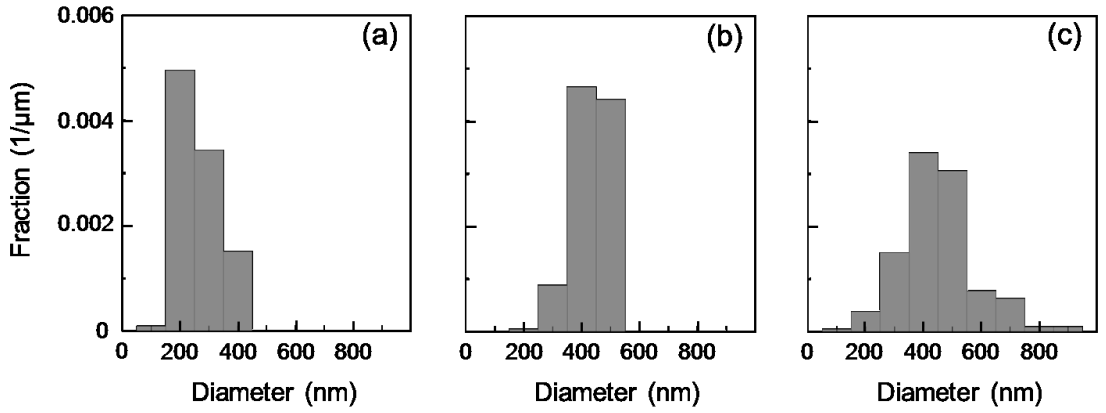

Figure 3.3. The distribution of the diameters of short fibers fabricated from polymer solutions with various concentrations: (a) 13 wt %, (b) 14 wt %, and (c) 15 wt %. The voltage was 5.5 kV, and the flow rate was 0.1 μL/min.

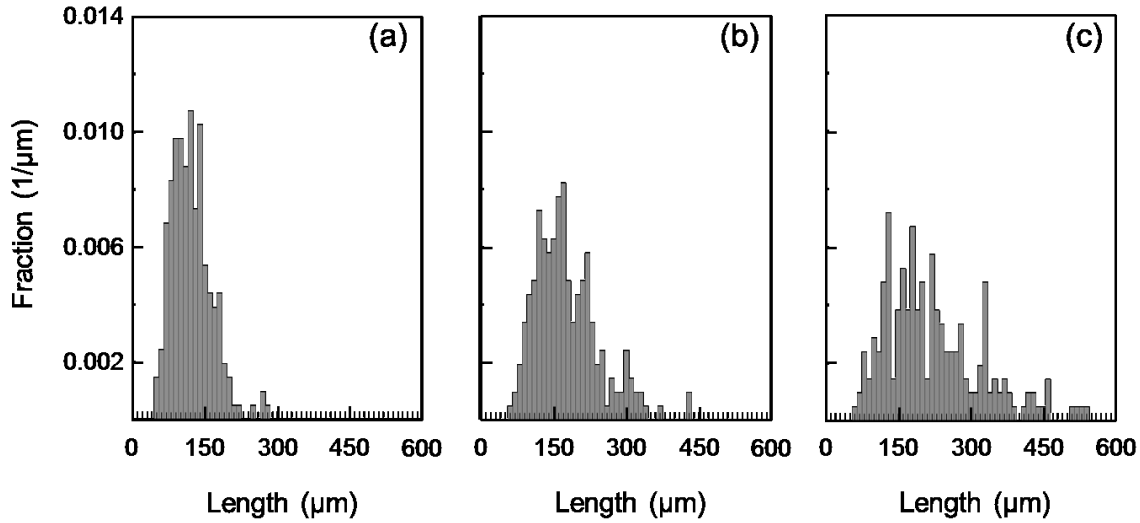

Figure 3.4. The distribution of the length of short fibers from polymer solutions with various concentrations: (a) 13 wt.%; (b) 14 wt.% ; (c) 15 wt.%. The voltage was 5.5 kV, and the flow rate was 0.1 μL/min.

When short nanofibers fabricated from polymer concentrations of 13, 14 and 15 wt. % were compared at a voltage of 5.5 kV and a flow rate of 0.1 μL/min, the 13 wt. % polymer solution produced a shorter length and a smaller diameter with a distribution of length and diameter that was more narrow, as shown in **Figures 3.3** and **3.4**. From these

results, the capability to control the length of short nanofibers was further investigated using a 13 wt. % polymer solution.

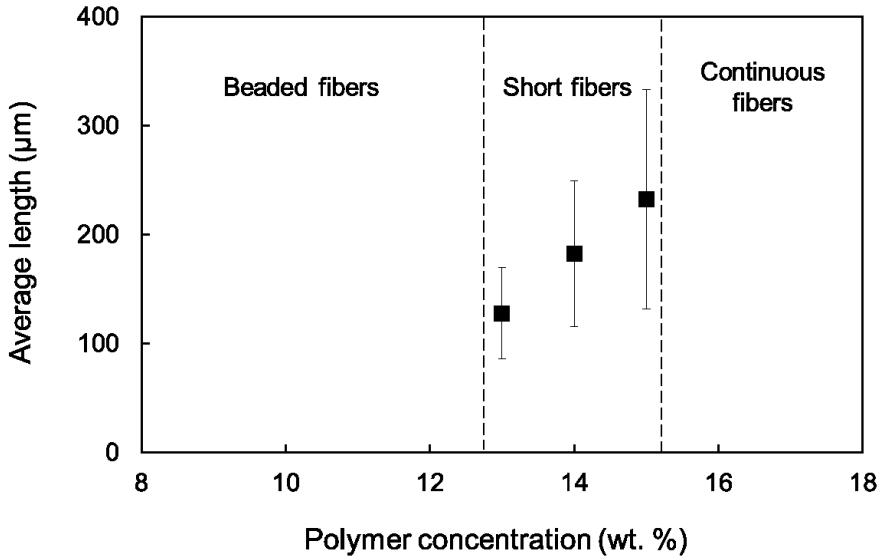

Figure 3.5. The average length of short nanofibers fabricated from polymer solutions with various concentrations. The voltage was 5.5 kV, and the flow rate was 0.1 μL/min. The morphologies of the fabricated fibers are indicated in the Figure

3.3.2. The effect of flow rate and voltage on fiber length of short nanofibers

The effect of flow rate and voltage on the length of short nanofibers was investigated using polymer solutions with concentrations of 13 wt. %.

The flow rate was varied from 0.01 to 0.7 μL/min, and the voltage was maintained at 5.5 kV. **Figure 3.6** shows the optical micrograph of short nanofibers fabricated at flow rates of 0.02, 0.08 and 0.4 μL/min. A few short nanofibers were found with a flow rate of 0.02 μL/min and an average length of short nanofibers of 65 μm (**Figure 3.6a**). At a flow rate of 0.08 μL/min, the average length was 120 μm and the production of short fibers was increased (**Figure 3.6b**). As the flow rate increased to 0.4 μL/min, the average length was 150 μm, and the production of short fibers was further

increased as the flow rate was increased (**Figure 3.6c**). The short nanofibers fabricated under these conditions were mostly straight in shape, although the flow rate was largely changed.

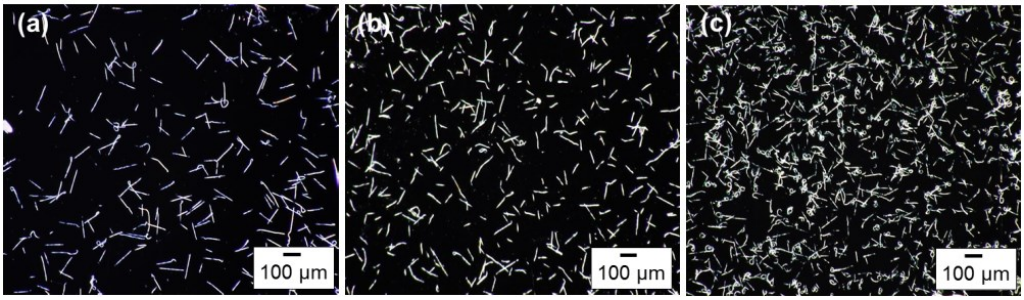

Figure 3.6. Optical micrograph of short nanofibers fabricated at various flow rates: (a) 0.02 µL/min; (b) 0.08; and, (c) 0.4 µL/min. The polymer concentration was 13 wt. %, and the voltage was 5.5 kV.

Figure 3.7 shows the average lengths of short nanofibers fabricated at flow rates ranging from 0.02 to 0.48 µL/min. At a flow rate of 0.01 µL/min, no short nanofibers could be fabricated, since the solution on the needle tip was freezing quickly and blocked the needle hole due to a low solution transfer. As the flow rate increased from 0.02 to 0.06 µL/min, the average length increased proportionally from 65 to 130 µm. At a flow rate range of 0.07-0.48 µL/min, the slope of the average length increment of short nanofibers was low, and the length of short nanofibers at 0.48 µL/min was increased to 170 µm. Short fibers could not be fabricated above a flow rate of 0.50 µL/min, but continuous fibers could. Thus, the length of nanofibers could be controlled by changing the flow rate, and straight fibers could be fabricated by applying voltage as high as 5.5 kV, as shown in **Figure 3.2**.

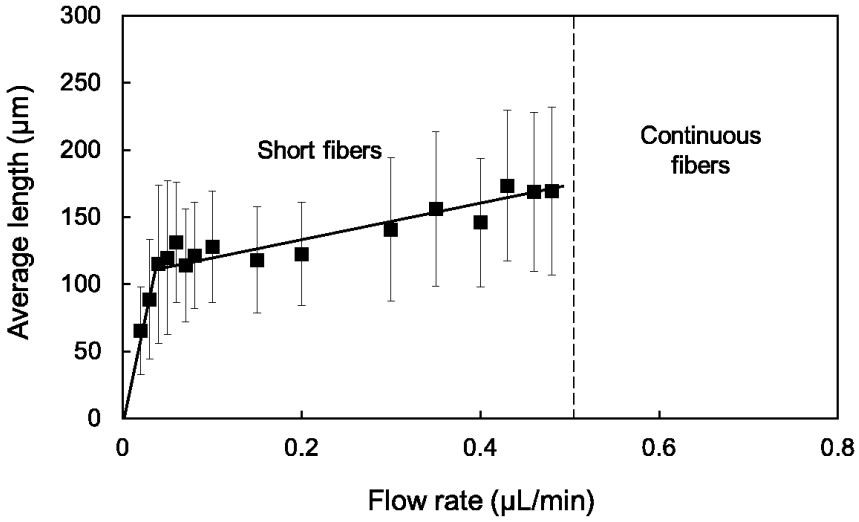

Figure 3.7. The average length of short nanofibers at various flow rates. The polymer concentration was 13 wt. % and the voltage was 5.5 kV. The morphologies of the fibers for each range are described in the figure.

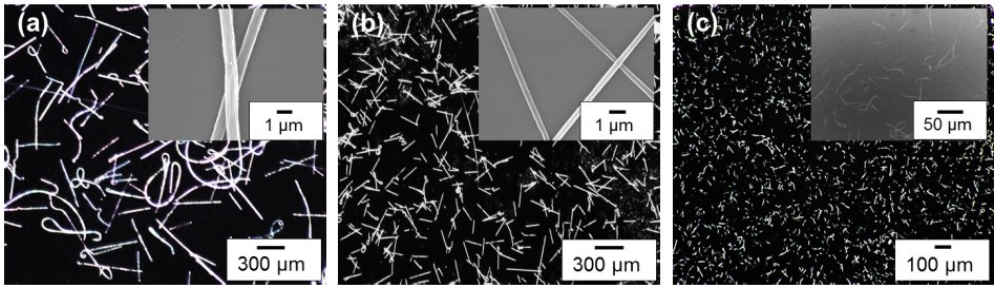

Figure 3.8. Optical micrograph of short nanofibers at various voltages: (a) 4.5 kV; (b) 4.7 kV; and, (c) 7.0 kV. The flow rate was 0.1 μL/min, and the polymer concentration was 13 wt. %.

The electrospinning of a 13 wt. % polymer solution was conducted at a flow rate of 0.1 μL/min, and the voltage was varied gradually from 0 to 12.0 kV. **Figure 3.8** shows the optical micrograph of short nanofibers fabricated at voltages of 4.5, 4.7 and 7.0 kV, respectively. **Figure 3.9** shows the relationship between average length and voltage. When the voltage was increased from 0 to 4.0 kV, a polymer solution jet could not be drawn by the electric field, so the fibers could not be fabricated. At a voltage of 4.5 kV, long discrete fibers with an average length of 670 μm could be fabricated

(**Figure 3.8a**). The average diameter of a short nanofiber was 750 nm, and the fibers had a curled shape that was caused by the weak stretching force from the applied voltage. When the voltage was increased to 4.7 kV, short nanofibers 380 nm in diameter could be fabricated, and the average length of the short nanofibers was decreased rapidly to 250 μm (**Figure 3.8b**). As the voltage was varied from 4.9 to 5.5 kV, the average length of short nanofibers ranged from 170 to 127 μm. The length of short nanofiber was almost constant at a voltage of 6.0 to 8.5 kV. The average length of short nanofibers fabricated at a voltage of 7 kV was 40 μm with a straight shape (**Figure 3.8c**). Above a voltage of 8.5 kV, the nanofibers could not be fabricated due to the imbalance between fibers drawn by the strong electric field and a low flow rate.

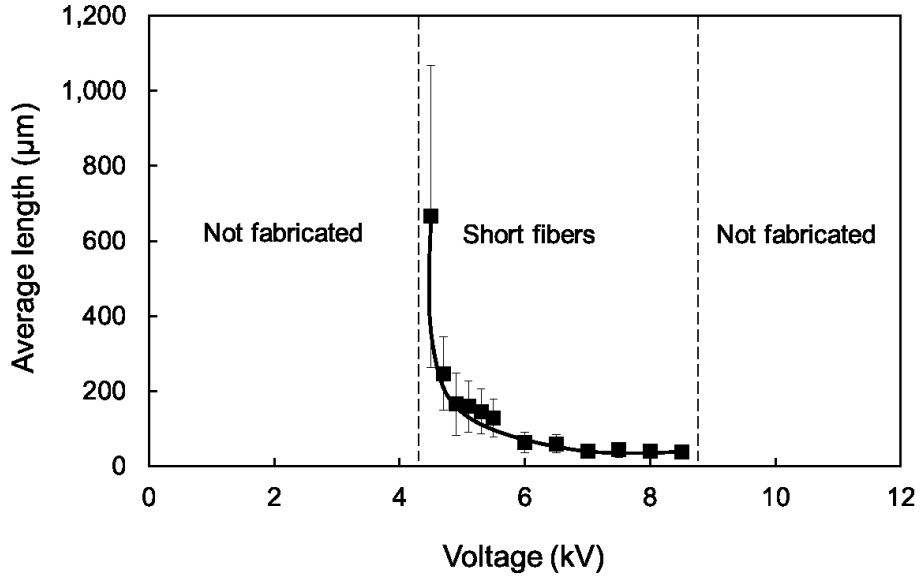

Figure 3.9. The morphologies and average lengths of fibers at various voltages and a flow rate of 0.1 μL/min for 13 wt. % polymer solutions.

Consequently, it was confirmed that the concentration of the polymer in the solution was the most important factor in the fabrication of short nanofibers. Short nanofibers could be fabricated using a 13 to 15 wt. % polymer solution. Using 13 wt. % of polymer solution, the length of short nanofibers could be controlled in a range of

from 65 to 170 μm (**Figures 3.6**, **3.7**) by altering the flow rate of the polymer solution, whereas the length could be controlled in a range of from 37 to 670 μm by altering the applied voltage (**Figures 3.8**, **3.9**). However, the diameter of fibers fabricated by applying low voltage was large and the shape was curled, although the short fibers were longer in length. When the voltage was increased, a straight short nanofiber could be fabricated.

3.3.3. Mechanism for the formation of short nanofiber

The fabrication mechanism for short nanofibers is discussed here based on the observation of short nanofibers and on the conditions of electrospinning. **Figure 3.10** shows the morphology of a typical short nanofiber fabricated at a flow rate 0.1 μL/min with a voltage of 5.5 kV.

The **Figure 3.10** compares the center (**Figure 3.10b**) with the edges (**Figures 3. 10cd**) of a short nanofiber. The diameter of the center portion ranged from 120 to 210 nm (**Figure 3. 10b**). The diameters of both edges of the short nanofiber were narrower than the diameter of the center portion, and it was stretched to approximately 70 nm in portions to within a range of 3 μm from the edge. This indicates that the fiber was locally stretched, leading to a thinning of the diameter of the fiber and to a breakaway of the fiber. This was due to the repulsive force of the surface charges and longitudinal force by the external electric field [33].

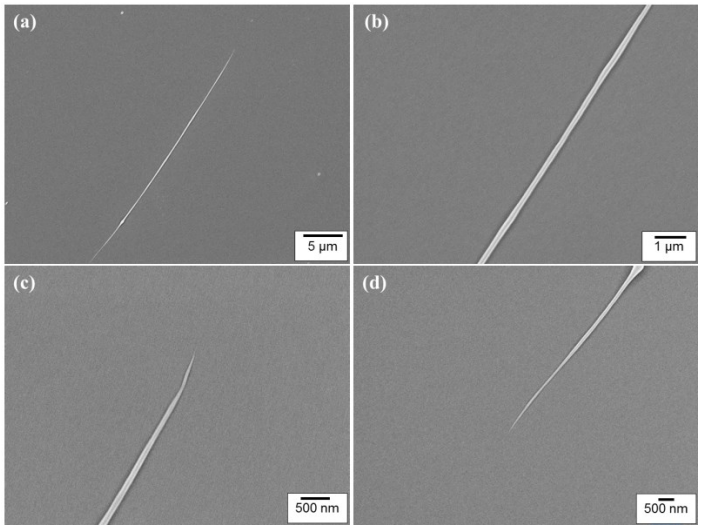

Figure 3.10. Typical short nanofibers fabricated from a 13 wt. % polymer solution: (a) a short nanofiber; (b) the center portion; (c) the upper-edge portion; and, (d) the lower-edge portion. The voltage was 5.5 kV, and the flow rate was 0.1 μL/min.

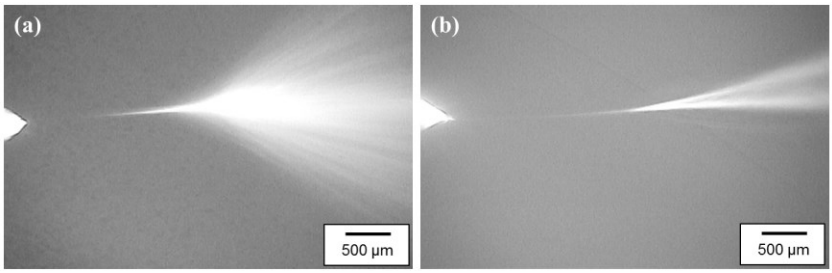

Figure 3.11. Polymer solution jets ejected from a needle tip: (a) a 9 wt. % polymer concentration (beaded fibers were fabricated); and, (b) a 13 wt. % polymer concentration (short nanofibers were fabricated). The voltage was 5.5 kV, and the flow rate was 0.3 μL/min.

The condition of the polymer solution jet that ejected from the needle tip was observed in order to determine the point at which the fibers were broken away. **Figure 3.11** shows the conditions of polymer solution jets with polymer concentrations of 9 and 13 wt. %, at which beaded fibers and short nanofibers were fabricated, respectively. During the fabrication of continuous fibers, a polymer solution jet generally maintains a straight path for some distance and then adopts a spinning and more complex path [33]. However, polymer solution jets at polymer concentrations of 9 and 13 wt. % have

straight segments of approximately 2 mm in length, and are then spread to angles of 37^{o} and 15^{o}, respectively. The spreading was due to a lateral perturbation caused by the repulsive forces between surface charges of the electrified polymer solution jet [33]. This must be a feature of fabrication of short nanofibers that leads to the breakaway of fibers. The difference in the spread angles for these two conditions was caused by the viscosity of the polymer solution that in turn was caused by the differences in the polymer concentration. When the polymer concentration was 9 wt. %, the spread angle of the polymer solution jet was wide due to low viscosity, and beads formed on the fibers due to a lack elasticity in the polymer solution jet [30]. When the polymer concentration was 13 wt. %, the solution was also broken away by the longitudinal force of an external electric field, although the spread angle of the polymer solution was relatively narrow due to the higher viscosity. However, the polymer solution was difficult to move in the solution jet, which resulted in short nanofibers with stretched edges, as shown in **Figure 3.10**.

Based on observation of the short nanofibers (**Figure 3.10**), on the condition of the polymer solution jets from the needle tip (**Figure 3.11**), and on the theoretical report [32-34], the major factor that led to the fabrication of the short nanofibers was the balance between the tensile strength of the polymer solution, the longitudinal force, and the lateral perturbation of the surface charge on the polymer solution jet. **Figure 3.12** shows the mechanism for short nanofiber fabrication and a diagram of the force in the straight pass after ejection and at the point of breaking. Eq. 1 describes these factors under equilibrium conditions on the cross-section area of the polymer solution jet,

$$F_t = \Delta F \cos\theta + F_L \quad (1)$$

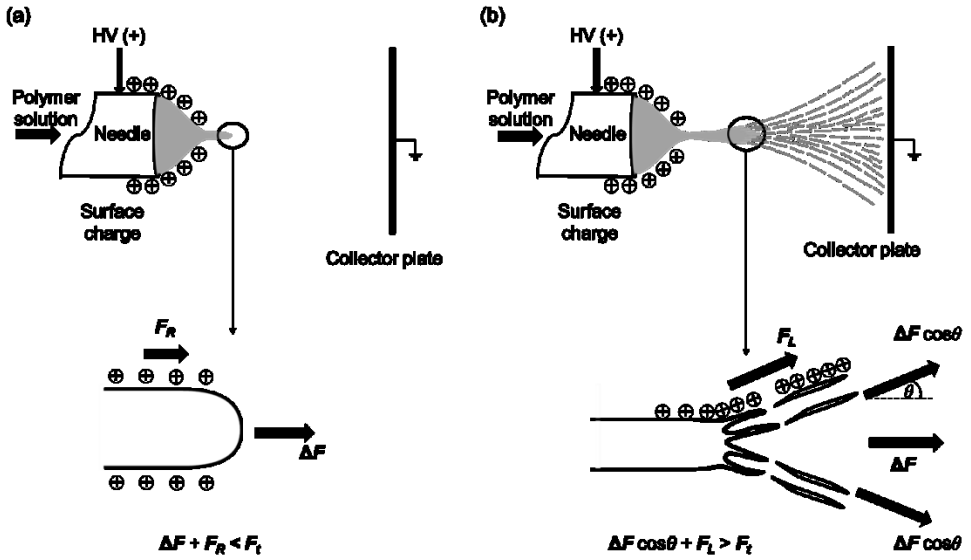

Figure 3.12. Diagram for the force of the polymer solution jet: (a) a straight pass after ejection; and, (b) at the breaking point.

where the tensile strength, F_t, is the maximum force that a polymer solution jet can withstand while being stretched before breaking. This force was affected by the mutual attraction of the polymer molecules and the polymer-solvent interaction in the polymer solution jet [20]. The high concentration of polymer could increase the mutual interaction of polymer molecules, and, thus, the tensile strength increased, whereas the selection of a solvent with a low surface tension could decrease the tensile strength. ΔF is the force in the longitudinal direction due to the applied voltage. The F_L is the force due to the repulsive force, F_R, between equal surface charges, which generates lateral perturbation [33,34]. The angle θ is measured from the jet axis. The polymer solution jet in the straight pass after ejection had a thick diameter with a straight shape and was flowing in a single path. The ΔF of the applied voltage and the repulsive force F_R of the surface charge on the polymer solution jet stretched the polymer solution jet and moved it forward (**Figure 3.12a**). In the straight path just before the jet was spread, the polymer solution jet could not break away, because it had a thick diameter and the ΔF and

repulsive force F_R of the surface charge were insufficient to break the polymer solution jet ($\Delta F + F_R < F_t$). As the polymer solution jet moved farther away, its diameter thinned, and the increase in the surface charge density resulted in an increase in the repulsive force F_R. The rapid increased in F_R generated a lateral perturbation, F_L, that made the polymer solution jet spread. Thus, short nanofibers were fabricated by the breaking of the fibers due to the resultant force of F_L, and the $\Delta F \cos\theta$ surpassed the tensile strength of the polymer solution jet ($\Delta F \cos\theta + F_L > F_t$) (**Figure 3.12b**).

3.5. Conclusions

The simple and one-step process fabrication of short polymer nanofibers has been successfully developed based on electrospinning method. This proves that electrospinning either can make short or continuous nanofiber. A polymer solution was loaded into a syringe, and was then ejected by the application of high voltage. The effect of the concentration of the polymer solution, the applied voltage, and the flow rate of the polymer solution was investigated for its effect on the fabrication of short nanofibers, and the following results were obtained. The concentration of the cellulose acetate polymer in the solution was important factor which varied from 13 to 15 wt. %. The length of fibers was increased by increasing the flow rate of the solution, and it was decreased with an increase in applied voltage, resulting in controllable length of short nanofibers at 37 to 670 μm. The edges of the short nanofibers were narrowed by stretching. Observation of the polymer solution jet that was ejected from the needle tip showed it passing straight, and then spreading due to lateral perturbations on its surface. The breaking of the fibers into short nanofibers occurred because the repulsive force

from the surface charges and the longitudinal force from the applied voltage surpassed the tensile strength of the polymer solution jet.

3.6. References

[1] J.N. Coleman, U. Khan, Y.K. Gun'ko, Mechanical reinforcement of polymers using carbon nanotubes, Adv. Mater. 18 (2006) 689-706.

[2] L.N. Song, M. Xiao, X.H. Li, Y.Z. Meng, Short carbon fiber reinforced electrically conductive aromatic polydisulfide/expanded graphite nanocomposites, Mater. Chem. Phys. 93 (2005) 122-128.

[3] B. Yao, G. Wang, J. Ye, X. Li, Corrosion inhibition of carbon steel by polyaniline nanofibers, Mater. Lett. 62 (2008) 1775-1778.

[4] S.A. Gordeyev, J.A. Ferreira, C.A. Bernardo, I.M. Ward, A promising conductive material: highly oriented polypropylene filled with short vapor-grown carbon fibres, Mater. Lett. 51 (2001) 32-36.

[5] E. Hablot, R. Matadi, S. Ahzi, L. Averous, Renewable biocomposites of dimmer fatty acid-based polyamides with cellulose fibres: Thermal, physical, and mechanical properties, Composites Sci. and Technol. 70 (2010) 504-509.

[6] S.Y. Fu, B. Lauke, E. Mader, C.Y. Yue, X. Hu, Tensile properties of short-glass-fiber- and short-carbon-fiber-reinforced polypropylene composites, Compos.: Part A Appl. Sci. Manuf. 31 (2000) 1117-1125.

[7] J. Huang, R.B. Kaner, A general chemical route to polyaniline nanofibers, J. Am. Chem. Soc. 126 (2004) 851-855.

[8] A.E. Deniz, A. Celebiouglu, F. Kayaci, T. Uyar, Electrospun polymeric nanofibrous composites containing TiO_2 short nanofibers, Mater. Chem. Phys. 129 (2011) 701-704.

[9] V.C. Li, K.H. Obla, Effect of fiber length variation on tensile properties of carbon-fiber cement composites, Compos. Eng. 4 (1994) 947-964.

[10] J.L. Thomason, The Influence of fiber length and concentration on the properties of glass fibre reinforced polypropylene: 5. Injection moulded long and short fibre PP, Compos. Part A Appl. Sci. Manuf. 33 (2002) 1641-1652.

[11] H. Zhang, Z. Zhang, K. Friedrich, Effect of fiber length of wear resistance of short carbon fiber reinforced epoxy composites, Compos. Sci. Technol. 67 (2007) 222-230.

[12] F. Rezaei, R. Yunus, N.A. Ibrahim, Effect of fiber length on thermomechanical properties of short carbon fiber reinforced polypropylene composites, Mater. Design 30 (2009) 260-263.

[13] M.H. Al-Saleh, U. Sundararaj, Review of mechanical properties of carbon nanofiber/polymer composites, Composites: Part A 42 (2011) 2126-2142.

[14] M. Endo, Y.A. Kim, T. Hayashi, K. Nishimura, T. Matusita, T. Mayashita, M.S. Dresselhaus, Vapor-grown carbon fiber (VGCFs) basic properties and their battery applications, Carbon 39 (2001) 1287-1297.

[15] G.G. Tibbetts, M.L. Lake, K.L. Strong, B.P. Rice, A review of vapor-grown carbon nanofiber/polymer composites, Compos. Sci. Technol. 67 (2007) 1709-1718.

[16] A. Stoiljkovic, S. Agarwal, Short electrospun fibers by UV cutting method, Macromol. Mater. Eng. 293 (2008) 895-899.

[17] C. Yoshikawa, K. Zhang, E. Zawadzak, H. Kobayashi, A novel shortened electrospun nanofiber modified with a 'concentrated' polymer brush, Sci. Technol. Adv. Mater. 12 (2011) 1-7.

[18] D. Li, Y. Xia, Electrospinning of nanofibers: Reinventing the wheel?, Adv. Mater. 16 (2004) 1151-1170.

[19] C.J. Luo, M. Nangrejo, M. Edirisinghe, A novel method of selecting solvents for polymer electrospinning, Polymer 51 (2010) 1654-1662.

[20] C.J Luo, E. Stride, M. Edirisinghe, Mapping the influence of solubility and dielectric constant on electrospinning polycaprolactone solutions, Macromolecules 45 (2012) 4669-4680.

[21] C.J. Luo, E. Stride, S. Stoyanov, E. Pelan, M. Edirisinghe Electrospinning short polymer micro-fibres with average aspect ratios in the range of 10-200, J. Polym. Res. 18 (2011) 2515-2522.

[22] I.W. Fathona, A. Yabuki, One-step fabrication of short electrospun fibers using an electric spark, J. Mater. Proces. Technol. 213 (2013) 1894-1899.

[23] S. Mahalingam, M. Edirisinghe, Forming of polymer nanofibers by a pressurised gyration process, Macromol. Rapid Commun. 34 (2013) 1134–1139.

[24] R. Konwarh, N. Karak M. Misra, Electrospun cellulose acetate nanofibers: The present status and gamut of biotechnological applications, Biotechnol. Adv. 31 (2013) 421-437.

[25] S. Tungprapa, T. Puangparn, M. Weerasombut, I. Jangchud, P. Fakum, S. Semongkhol, C. Meechaisue, P. Supaphol, Electrospun cellulose acetate fibers: effect of solvent system on morphology and fiber diameter, Cellulose 14 (2007) 563-575.

[26] N. Bhardwaj, S.C. Kundu, Electrospinning: A fascinating fiber fabrication technique, Biotechnol. Adv. 28 (2010) 325-347.

[27] Z.M. Huang, Y.Z. Zhang, M. Kotaki, S. Ramakrishna, A review on polymer nanofibers by electrospinning and their applications in nanocomposites, Compos. Sci. Technol. 63 (2003) 2223-2253.

[28] J.Y. Chen, H.C. Chen, J.N. Lin, C. Kuo, Effects of polymer media on electrospun mesoporous titania nanofibers, Mater. Chem. Phys. 107 (2008) 480-487.

[29] K.H. Lee, H.Y. Kim, H.J. Bang, Y.H. Jung, S.G. Lee, The change of bead morphology formed on electrospun polystyrene fibers, Polymer 44 (2003) 4029-4034.

[30] J.H. Yu, S.V. Fridrikh, G.C. Rutledge, The role of elasticity in the formation of electrospun fibers, Polymer 47 (2006) 4789-4797.

[31] S.L. Shenoy, W. Douglas, B.H.L. Frisch, G.E. Wnek, Role of chain entanglements on fiber formation during electrospinning of polymer solutions: good solvent, non-specific polymer–polymer interaction limit, Polymer 46 (2005) 3372-3384.

[32] D.H. Reneker, A.L. Yarin, H. Fong, S. Koombhongse, Bending instability of electrically charged liquid jet of polymer solutions in electrospinning, J. Appl. Phys. 87 (2000) 4531-4547.

[33] M.M. Hohman, M. Shin , G. Rutledge, M.P. Brenner, Electrospinning and electrically forced jets. I. Stability theory, Phys. Fluids 13 (2001) 2201-2220.

[34] M.M. Hohman , M. Shin , G. Rutledge, M.P. Brenner, Electrospinning and electrically forced jets. II. Applications, Phys. Fluids 13 (2001) 2221-2236.

Chapter 4

One-step fabrication of short nanofibers by electrospinning: Effect of needle size on nanofiber length.

4.1. Introduction

Recently, researches on short fibers have been performed intensively due to its ability to enhance the tensile strength, conductivity, corrosion resistance, and thermal stability of the polymer composite for many applications, for example, aerospace, automotive industries, corrosion protection, flexible display, or electrode, etc. [1-4]. Electrospinning has been employed by several researchers to produce fibers due to its simple process. However, the post processing are always needed to produce the short fibers from the as spun continuous fibers. Stoiljkovic et al. have used the concept of a photocross-linking reaction upon UV radiation as a secondary process [5], whereas Yoshikawa et al. have employed the mechanical cutting of electrospun fibers dispersed in the water using homogenizer as secondary process [6]. The direct fabrication of short fibers using electrospinning method has been reported and performed [7,8]. Luo et al. have reported the direct fabrication of short micro-fibers with aspect ratio of 10-200 by altering the molecular weight of polymethylsisesquioxane (PMSQ) and using the volatile solvent [7]. In the chapter 2, the electric spark was utilized to cut the fibers during electrospinning [8].

In this chapter, a one-step process for the production of short polymer nanofibers using an electrospinning technique is proposed. Differing from our previous work which describe in chapter 2 [8], the electric spark generator was uninstalled from the electrospinning setup. The polymer solution was loaded into a syringe with a needle,

and then it was ejected by applying a high-voltage. The short fibers were produced and theirs length could be controlled by changing the needle size. The obtained short nanofibers were investigated by measuring the diameter and the length. The mechanism of formation of short nanofibers is described and a simple theoretical model is proposed.

4.2. Experimental

4.2.1. Preparation and electrospinning of the polymer solution

Cellulose acetate (CA, Sigma Aldrich, UK) with a number-average molecular weight of 30,000 was used. The solvent was a mixture of acetone (Kanto Chemical, Japan) and N,N-dimethyl acetamide (DMAc) (Wako Chemical, Japan) at a volume ratio of 2:1. The total weight fraction of CA in the solution was set at 13 wt. %. The mixture of CA powder and solvent in the closed bottle was stirred using a magnetic stirrer until a homogeneous solution was obtained. The conventional horizontal set up of electrospinning was used to fabricate polymer short nanofibers. The polymer solution was loaded into a 1,000 cc syringe with various stainless needle size of N26 (OD: 0.46 mm, ID: 0.26 mm), N30 (OD: 0.31 mm, ID: 0.16 mm), and N32 (OD: 0.23 mm, ID: 0.11 mm) . The voltage of 4.5 kV was obtained from high-voltage power supply (HER-15P5-LV, Matsusada Precision Inc.). The flow rate of polymer solution was controlled from 0.1 to 0.5 μL/min by a syringe pump (ESP64, EiCom Corporation). An aluminum plate of 30 mm x 30 mm as a fibers collector was connected to the ground and the distance between the needle tip and the aluminum plate was set to 90 mm. The ambient temperature and humidity were maintained at 20 ºC and 60% using an integrated humidifier and temperature controller (PAU-300S, Apiste Corporation).

4.2.2. Observation of short nanofibers

The prepared short nanofibers were observed by SEM (JSM-6340F, JEOL Ltd.) with an acceleration voltage of 20 kV. The shape of the short fibers was evaluated by measuring the diameter at the centers and the edges of the fibers. The lengths and diameters of the short nanofibers were measured using the ruler function of image processing software during observation using a digital microscope with a resolution of 2.11 MP (VH-8000, Keyence Corporation) and a high-range zoom lens with a magnification ranging from 450 - 3,000x (VH-Z450, Keyence Corporation).

4.3. Results and discussion

4.3.1. Effect of needle size on the fiber diameter and length

The electrospun fibers were fabricated from a polymer solution of 13 wt. % concentration, and the morphology of the fibers was observed. Three needles with different inner diameter of N26, N30, and N32 were used. The fiber jet could be drawn at voltage of 4.5 kV, and the flow rate of the polymer solution was varied gradually from 0.1 to 0.5 μL/min. As results, two types of morphologies of fibers were recognized: the short nanofibers were fabricated at flow rate ranging from 0.1 to 0.48 μL/min and continuous fibers were fabricated at flow rate 0.5 μL/min. For further investigation, a voltage of 4.5 kV and flow rate of 0.1 μL/min were employed.

Figures 4.1a, **4.1b**, and **4.1c** show the optical micrographs and SEM images of the short nanofibers fabricated from different needles of N26, N30, and N32, respectively. As the needle inner diameter was increased from 0.16 to 0.26 mm, which is N30 and N26, the averages diameter of short fibers were increased approximately twice, that is from 170 to 370 nm. At the N32 the average short fiber diameter was 168

nm. **Figure 4.2** shows the distributions of the lengths of the short nanofibers produced from various needles. The short nanofibers fabricated from the needle of N26 had an average length of 123 μm with a broad distribution (**Figure 4.2a**). As the needles of N30 and N32 were employed, the average length decreased to 80 and 50 μm, respectively, and the distributions were narrow (**Figures. 4.2b** and **4.2c**). The average length of short nanofibers was increased 1.6× as inner diameter of needle was increased with the factor 1.5 (N30/N32) and 1.6 (N26/N30).

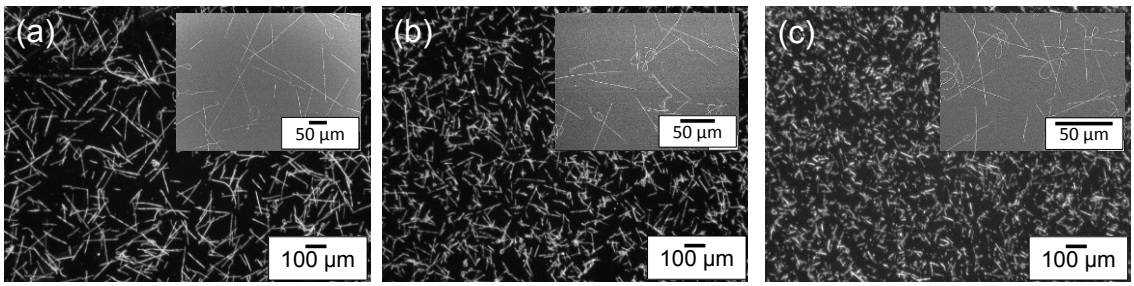

Figure 4.1. Optical micrographs and SEM images of short nanofibers fabricated at various needle sizes: (a) N26; (b) N30; and, (c) N32.

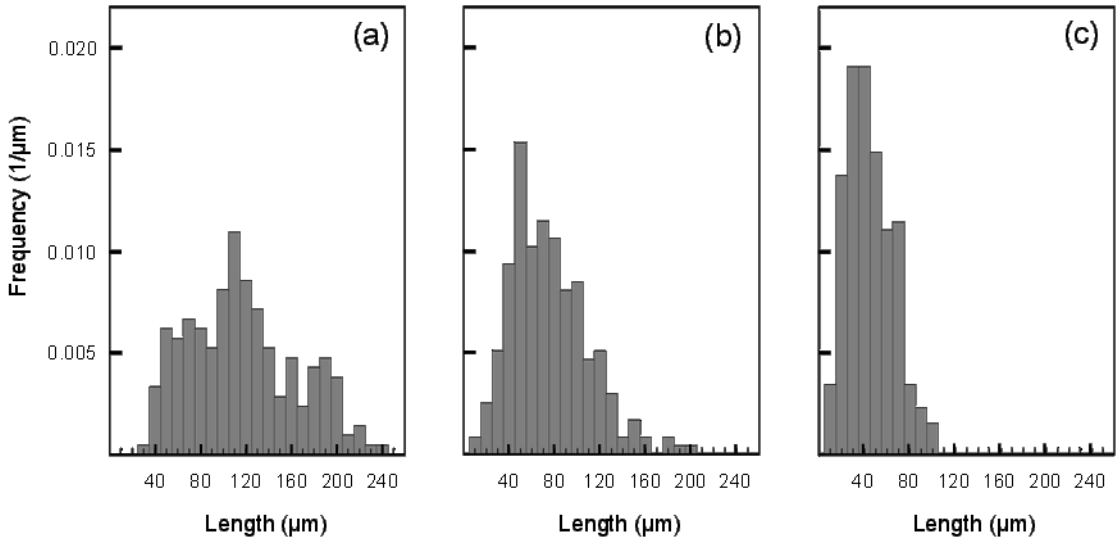

Figure 4.2. The distribution of the lengths of short fibers fabricated at various needles: (a) N26; (b) N30; and, (c) N32.

4.3.2. Mechanism formation of short nanofibers

Figure 4.3a shows the morphology of a typical short nanofiber fabricated using the needle of N26 at a flow rate 0.1 μL/min and a voltage of 4.5 kV. The shape of the center (**Figure 4.3b**) and the edges (**Figures. 4.3c** and **4.3d**) of a short nanofiber was compared. The diameter of the center portion ranged from 270 to 360 nm. The diameters of both edges of the short nanofiber were narrower than that of the center portion, and it was stretched to approximately 90 nm in portions within a range of 1 μm from the edge. This indicates that the fiber was locally stretched, leading to a thinning of the diameter of the fiber and to a breakaway of the fiber. This was due to the longitudinal force by the external electric field [9].

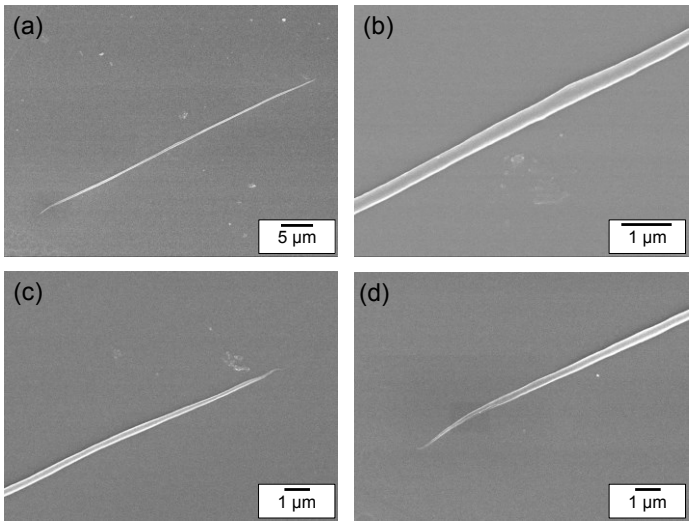

Figure 4.3. Typical short nanofibers fabricated from a needle of N26: (a) a short nanofiber; (b) the center portion; (c) the upper-edge portion; and, (d) the lower-edge portion.

The major factor that led to the fabrication of the short nanofibers is the balance between the force of the surface tension of the polymer solution, the longitudinal force, and the lateral perturbation on the surface of the polymer solution jet. **Figure 4.4**

represents the mechanism for short nanofiber fabrication. Eq. 1 describes these factors under equilibrium conditions,

$$\pi R\sigma=\Delta F \quad (1)$$

where the surface tension σ is the cohesive force of the polymer molecules on the surface with radius *R*. The term *ΔF* is the resultant force in the longitudinal direction that is the ratio between the Coulomb force, *Fq*, and the net cohesive force, *Fc*, in the polymer solution jet (*ΔF= Fq – Fc*). The polymer solution jet in the straight pass after ejection had a straight shape and was flowing in a single path. On the cross-section of this polymer solution jet, the *ΔF* slightly dominated the surface tension, so the polymer solution jet was stretched and moved forward (**Figure 4.4a**). In this straight path, the polymer solution jet could not break away, because it had a thick diameter of *R* which has almost same in size with inner diameter of needle. As the polymer solution jet moved further away, its diameter thinned with a large ratio becomes *r* and then the longitudinal force of the external electric field easily broke it. Thus, short nanofibers were fabricated by the breaking of fibers due to the significant imbalance of force between the surface tension of the polymer solution and the resultant influence of Coulomb force, *Fq* from the applied voltage, and the net cohesive force, *Fc*, of polymer molecule confined on the polymer solution jet (**Figure 4.4b**). From this mechanism, the broken fiber has correlation with the inner-diameter of needle, and the shorter fibers were fabricated from the smaller inner diameter of needle.

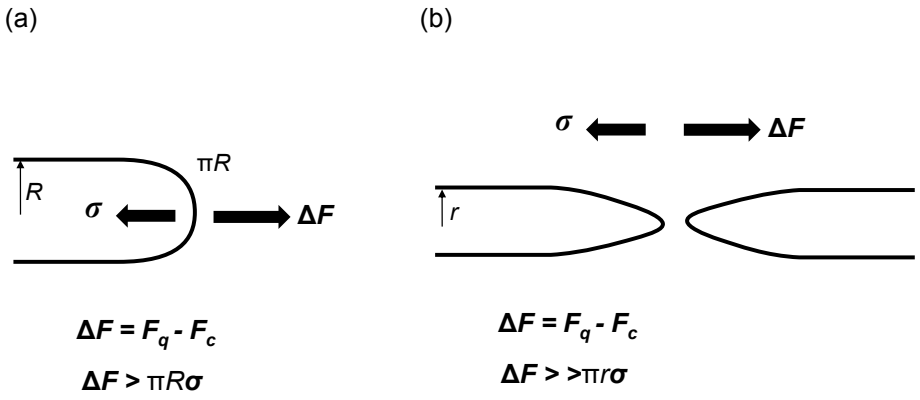

Figure 4.4. Diagram for the force of the polymer solution jet during the short nanofiber fabrication: (a) a straight pass after ejection; and, (b) at the breaking point.

4.4. Conclusions

The effect of the needle size on the length of nanofiber was investigated, and the following results were obtained. The short nanofiber average diameter was increased approximately twice, as the needle inner diameter was increased from 0.16 to 0.26 mm. The short nanofibers average length was increased with the factors 1.5-1.6×, as needle inner diameter was increased 1.6×. The edges of the short nanofibers were narrowed by stretching due to the longitudinal force of applied voltage. The breaking of the fibers into short nanofibers occurred due to an imbalance between the force of the surface tension of the polymer solution and the longitudinal force from the applied voltage.

4.5. References

[1] L.N. Song, M. Xiao, X.H. Li, Y.Z. Meng, Short carbon fiber reinforced electrically conductive aromatic polydisulfide/expanded graphite nanocomposites, Mater. Chem. Phys. 93 (2005) 122-128.

[2] B. Yao, G. Wang, J. Ye, X. Li, Corrosion inhibition of carbon steel by polyaniline nanofibers, Mater. Lett. 62 (2008) 1775-1778.

[3] S.A. Gordeyev, J.A. Ferreira, C.A. Bernardo, I.M. Ward, A promising conductive material: highly oriented polypropylene filled with short vapour-grown carbon fibres, Mater. Lett. 51 (2001) 32-36.

[4] E. Hablot, R. Matadi, S. Ahzi, L. Averous, Renewable biocomposites of dimmer fatty acid-based polyamides with cellulose fibres: Thermal, physical and mechanical properties, Compos. Sci. Technol. 70 (2010) 504-509.

[5] A. Stoiljkovic, S. Agarwal, Short electrospun fibers by UV cutting method, Macromol. Mater. Eng. 293 (2008) 895-899.

[6] C. Yoshikawa, K. Zhang, E. Zawadzak, H. Kobayashi, A novel shortened electrospun nanofiber modified with a 'concentrated' polymer brush, Sci. Technol. Adv. Mater. 12 (2011) 1-7.

[7] C.J. Luo, E. Stride, S. Stoyanov, E. Pelan, M. Edirisinghe, Electrospinning short polymer micro-fibres with average aspect ratios in the range of 10-200, J. Polym. Res. 18 (2011) 2515-2522.

[8] I.W. Fathona, A. Yabuki, One-step fabrication of short electrospun fibers using an electric spark, J. Mater. Proces. Technol. 213 (2013) 1894-1899.

[9] D.H. Reneker, A.L. Yarin, H. Fong, S. Koombhongse, Bending instability of electrically charged liquid jet of polymer solutions in electrospinning, J. Appl. Phys. 87 (2000) 4531-4547.

Chapter 5

Short electrospun composite nanofibers: Effects of nanoparticle concentration and surface charge on fiber length

5.1. Introduction

Research into composite fibers has recently intensified in various industrial fields. The presence of nanoparticles has resulted in an enhancement of the mechanical, photocatalytic, electrical, thermal, and optical properties of the fibers [1-16]. Nano-sized composite fibers can utilize the characteristic features of nanoparticles such as tunable electronic band gaps and a high surface area. Yu et al. have reported that the photoluminescent property of cadmium sulfate quantum-dots with a particle-size-dependent electronic band gap could be enhanced by embedding the cadmium quantum-dots into polyethylene oxide fiber [8]. This kind of material is expected to be applicable to the preparation of electroluminescent devices and nano-optoelectronic devices [8]. The photocatalytic efficiency of TiO_2 in the nanofiber morphology is highly superior to that of the TiO_2 film or nanoparticles [17,18]. The enhancement of photocatalytic efficiency is due to the high surface areas and high porosity of the TiO_2 nanofibers. The short fibers have several advantages compared to continuous fiber [19-21]. Anil et al. have reported using the short nanofibers as a drug carrier with a diameter and length of 4 nm and 50-400 nm, respectively, that could deliver the drugs to a tumor site within a much shorter period of time compared with that of a spherical nanoparticle [19]. Fu et al. report that the special regular short nanofiber microstructure has had a great impact on photocatalytic performance and removal efficiency, and that it greatly increases the

permeability of visible light, expands the reaction zone, and promotes photocatalytic efficiency [20]. Jiang et al. report that the short electrospun polyimide fiber dispersed in a polymer matrix enhances the mechanical properties of a polymer matrix with the addition of only 2 wt. % of short fiber, whereas the amount of continuously long polyimide fiber required to even approximate the mechanical strength was much higher as 38 wt. % [21]. Therefore, the studies of both effects of nanoparticles and processing parameters on the fabrication of short composite fibers are relevant in order to find the optimum performance of short composite fibers that could contribute to further research such as drug carriers, material templates for hollow or porous structures of metal oxide, membranes, and high tensile and modulus materials.

The method that is commonly used to fabricate short fibers is called the vapor-grown technique. With this technique, a controllable length of short fibers can be achieved by altering the catalyst size, temperature processing, and catalyst activity [22,23]. This technique is feasible for industrial applications; however, several drawbacks persist, such as an extended chemical route and post-processing, which are necessary in order to enhance the physical properties of the carbon fibers. A novel method to fabricate short fibers is called the pressurized gyration process, which combines centrifugal spinning and solution blowing [24]. With this process, the diameter and length of obtained fibers are 60-1000 nm and 200-800 mm, respectively. This method offers mass production capabilities, but the length of the nanofibers is too long for use as filler. These problems have motivated many researchers to find effective methods for the fabrication of short fibers or short composite fibers.

Electrospinning is a simple and reliable method for the fabrication of fibers with diameters in the nano to micro scale. A polymer solution is electrified by high voltage to

form a cone jet, which stretches to fabricate the nanofibers. Composite nanofiber can be produced with this technique by utilizing a suspension of polymer/nanoparticles as a precursor [25-27]. The nanofibers prepared via the electrospinning method are generally continuous, and secondary processes must be applied in order to fabricate short nanofibers. Ali et al. used mechanical crushing as a secondary process in order to fabricate TiO_2 short nanofibers from the continuous electrospun fibers of polyvinylpirrolidone/TiO_2 [28]. In the chapter 2 and 3, short electrospun polymer nanofibers could be fabricated in a one-step process. In these methods, the short nanofibers could be fabricated by cutting the continuous fibers using an electric spark [29], and by regulating the concentration of the polymer, the flow rate, and the working voltage [30]. One-step process methods of electrospinning can be applied to the fabrication of short composite nanofibers by replacing the polymer solution with a polymer/nanoparticle solution.

In this chapter, the polymer/nanoparticle solutions consisted of cellulose acetate, TiO_2 nanoparticles, and organic solvents that were electrospun to fabricate short composite nanofibers. The goal of this study was to investigate the effect of the concentrations and the surface charges of the nanoparticles on the length of fabricated short composite nanofibers that could contribute to the development of drug delivery systems, material template fabrication, and fibril filler for composite materials. The morphologies of the fabricated short composite nanofibers and the conditions of the electrospun jets of the polymer/nanoparticle solutions were observed to elucidate the mechanism of fabrication for short composite nanofibers.

5.2. Experimental methods

5.2.1. Preparation of the polymer/nanoparticle solutions

The polymer/nanoparticle solutions consisted of cellulose acetate polymer powder with a molecular weight of 30,000 (Sigma Aldrich, UK), TiO_2 nanoparticles with a diameter of 10-30 nm (TTO-51C (rutile type), Ishihara Sangyo Kaisha, Ltd., Japan), and organic solvents that consisted of acetone (>99.5%, Kanto Chemical, Japan) and N,N-dimethyl acetamide (DMAc) (>99.5%, Sigma Aldrich, UK) with a volume ratio of 2:1. The concentration of the polymer was set at 13 wt. % and the concentrations of TiO_2 nanoparticles in the polymer/nanoparticle solutions were varied from 0.5 to 17 wt. % for the fabrication of short composite nanofibers. The prepared polymer/nanoparticle solutions turned to short composite nanofibers with 4 to 56 wt. % nanoparticles after evaporation of the organic solvent. The suspension was prepared by pouring the TiO_2 nanoparticles into 15 mL of organic solvent, which was then subjected to an ultrasonic homogenizer in a closed bottle for 30 min. The polymer powder was added into the suspension of TiO_2 nanoparticles and organic solvent and then stirred and homogenized for 3 h. During the ultrasound-homogenization process, the weight of the suspension decreased as a portion of the organic solvent was evaporated. After dispersion, organic solvent was added to compensate for the weight loss of the suspension and to return the weight ratio of each component to the original amount. Polymer/nanoparticle solutions of various pHs were prepared using either aqueous sodium hydroxide or hydrochloric acid. The pH of the solution was measured using a digital pH meter (Cyberscan pH 110, EUTECH INSTRUSMENTS) with a glass electrode (EC620131, EUTECH INSTRUSMENTS). The viscosity of each solution was measured using a viscometer (TVE-22H cone plate type, Toki Sangyo Co., Ltd, Japan).

5.2.2. Electrospinning of the polymer/nanoparticle solutions

A conventional electrospinning setup was used to fabricate short composite nanofibers. The polymer/nanoparticle solutions were loaded into a 1,000 cc syringe (TTL 2-432, Hamilton Company) with a stainless needle (OD: 0.46 mm, ID: 0.26 mm). A high-voltage power supply (HER-15P5-LV, Matsusada Precision Inc.) was connected to the stainless needle to electrify the polymer/nanoparticle solutions. The voltage was increased gradually to find the appropriate voltage for conducting electrospinning. The flow rates of polymer/nanoparticle solutions were controlled via a micro syringe pump (ESP64, EiCom Corporation). The voltage and the flow rates were set at 5.5 kV and 0.1 μL/min, respectively [30]. A 30 mm x 30 mm aluminum plate that was used to collect the electrospun nanofibers was connected to the ground, and a 3 mm x 3 mm silicon wafer was attached to observe the nanofibers. The distance between the needle tip and the aluminum plate was set at 90 mm. The ambient temperature and humidity were maintained at 20 ºC and 60% using a temperature controller and an integrated humidifier (PAU-300S, Apiste Corporation), respectively.

5.2.3. Measurement of the zeta potential of TiO_2 nanoparticles

The zeta potential of the nanoparticles was measured at pH values ranging from 2 to 11 via a Nanozeta apparatus (Malvern Zetasizer, Nano ZS, UK). The TiO_2 nanoparticles were dispersed into 100 mL of deionized water with a concentration 0.05 wt. %. Then, 1 M of either aqueous sodium hydroxide or hydrochloride acid was dropped gradually into the solution to control the pH.

5.2.4. Observation of short composite nanofibers

The diameters and the lengths of fabricated short composite nanofibers were measured using the ruler function of image processing software during observation with a digital microscope at a resolution of 2.11 megapixels (VH-8000, Keyence Corporation). Two types of lenses, a low-range lens and a high-range zoom lens with a magnification ranging from 25-3,000x (VH-Z450, Keyence Corporation), were used for the observation. The distribution and the average lengths of the short composite fibers were determined for more than 200 fibers. The morphologies of the short composite nanofibers were observed using a scanning electron microscope (SEM) (JSM-6340F, JEOL Ltd.) with a maximum magnification factor of 650,000x and a resolution of 1.2 nm at an acceleration voltage of 20 kV.

The conditions of the electrospinning jets of various polymer/nanoparticle solutions were observed using a CCD camera with a resolution of 0.4 megapixels, twice-digital zoom, and 0.8 lux of minimum illumination (MTV-73x11HN, Mintron Enterprise Co., Ltd). A monocular optical lens with a diameter of 50 mm and a magnification factor of 8 (M0850, Specwell) was attached to the CCD camera. The images were taken at a speed of 30 fps and were recorded on a personal computer.

5.3. Results and discussion

5.3.1. The effect of nanoparticle concentration on the length of short composite nanofibers

We previously reported that short nanofibers could be fabricated using a 13 wt. % cellulose acetate polymer solution [29,30]. Therefore, 13 wt. % concentrations of polymer were chosen. **Figure 5.1** shows the short composite nanofibers with various

concentrations of nanoparticles fabricated by the electrospinning of a 13 wt. % polymer solution at a voltage of 5.5 kV and a flow rate of 0.1 μL/min. The short plain polymer nanofibers without nanoparticles were almost straight, although some curling was observed toward the ends of the short nanofibers (**Figure 5.1a**). The diameters of the short plain nanofibers ranged from 110 to 150 nm. The short composite nanofibers produced using a 4 wt. % concentration of nanoparticles were also straight and had a smooth surface—a few nanoparticles were observed on the surface of the fibers (**Figure 5.1b**). The diameters of the short composite nanofibers were larger, and ranged from 250 to 270 nm. The short composite nanofibers with a 5 to 7 wt. % concentration of nanoparticles showed morphologies that were similar to those produced using a 4 wt. % concentration of nanoparticles. The morphology of short composite nanofibers with a 38 wt. % concentration of nanoparticles was also straight and a bead was recognized on each of the short composite nanofibers (**Figure 5.1c**). Some nanoparticles were observed on the surface of the nanofibers. The diameters of short composite nanofibers with a 38 wt. % concentration of nanoparticles were larger, and ranged from 310 to 370 nm. The short composite nanofibers with a 40 to 50 wt. % concentration of nanoparticles had a similar morphology to the nanofibers with a 38 wt. % concentration of nanoparticles.

Figure 5.2 shows the distribution of the lengths of the short plain and composite nanofibers from **Figure 5.1**. The short plain polymer nanofibers and the short composite nanofibers with a 4 wt. % concentration of nanoparticles had an average length of 120 and 112 μm, respectively, with a broad distribution (**Figures 5.2ab**). As the concentration of nanoparticles was increased to 38 wt. %, the average length of the short composite nanofibers decreased to 47 μm, and the distribution narrowed **(Figure 5. 2c**).

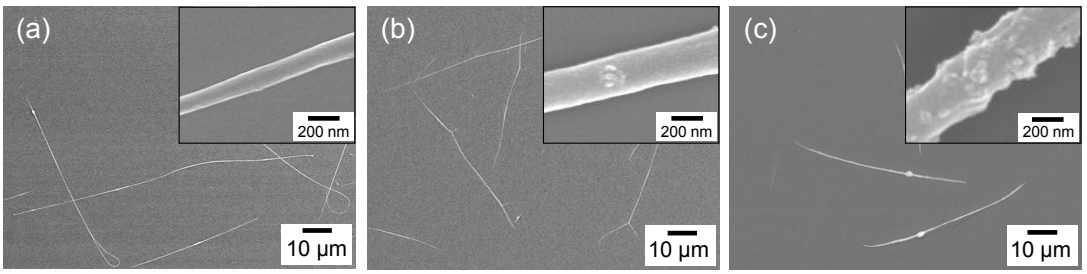

Figure 5.1. Short plain polymer nanofibers (a), and short composite nanofibers with TiO_2 nanoparticle concentrations of 4 wt. % (b) and 38 wt. % (c) fabricated with a voltage of 5.5 kV and a flow rate of 0.1 μL/min.

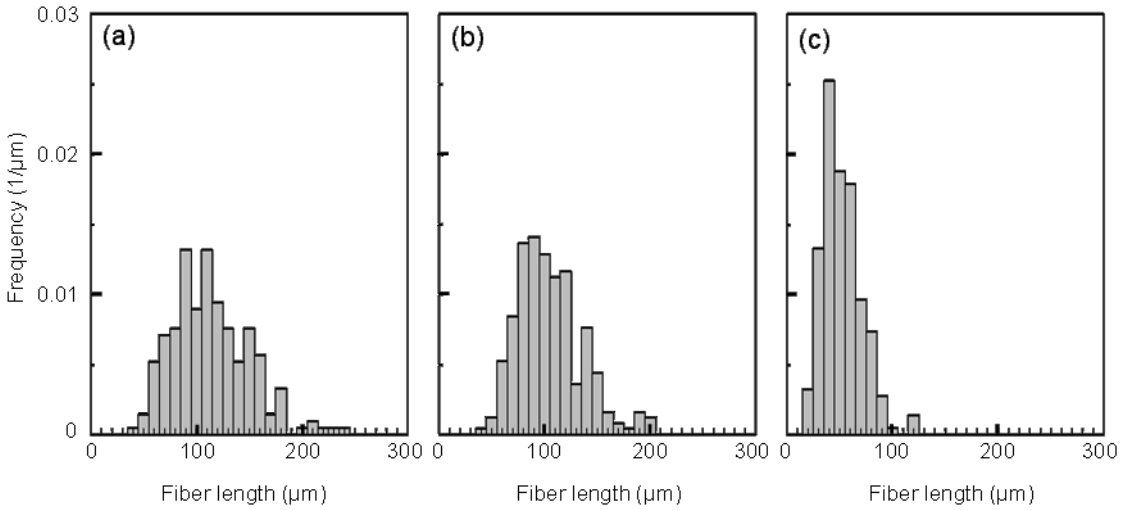

Figure 5.2. Distribution of the lengths of short plain nanofibers (a) and composite nanofibers with TiO_2 nanoparticle concentrations of 4 wt. % (b) and 38 wt. % (c) fabricated with a voltage of 5.5 kV and a flow rate of 0.1 μL/min.

Figure 5.3 shows the average lengths of short composite nanofibers fabricated from solutions with various nanoparticle concentrations. The average length of the short composite nanofibers was significantly decreased (from 112 to 70 μm) as the concentration of nanoparticles was increased from 4 to 5 wt. %. The average length of the short composite nanofibers with a 7 wt. % concentration of nanoparticles was approximately 60 μm, which gradually decreased to 40 μm for nanoparticle concentrations of 50 wt. %. The short composite nanofibers with a 56 wt. %

concentration of nanoparticles could no longer be electrospun. This was caused by the high viscosity of the solution. During the fabrication of short composite nanofibers, the threshold concentration for added nanoparticles that resulted in significant changes in fiber length was found to be 5 wt. %.

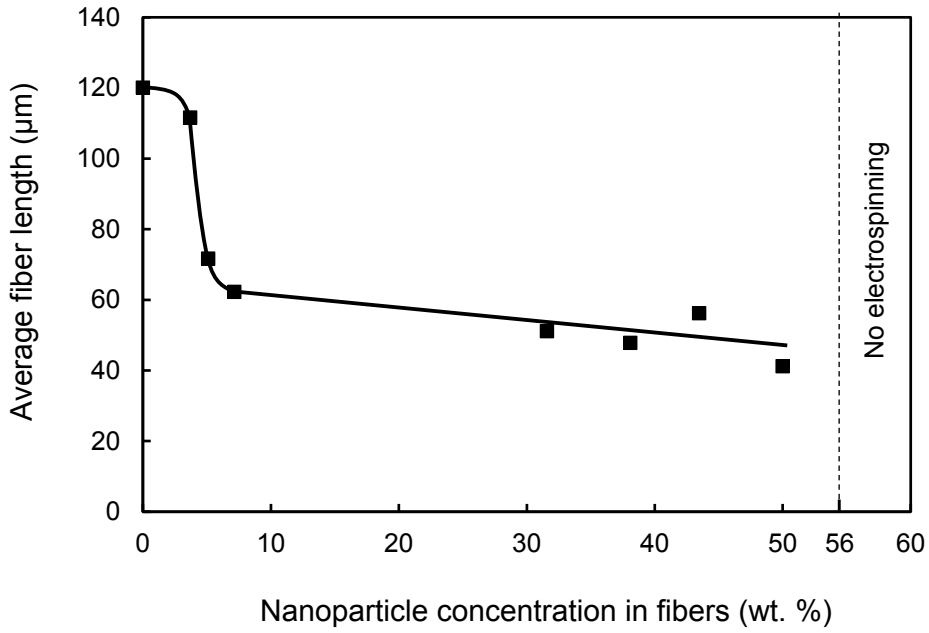

Figure 5.3. Average lengths of short composite nanofibers containing various nanoparticle concentrations.

The viscosities of the polymer/nanoparticle solutions with various nanoparticle concentrations are shown in **Figure 5.4**. The concentration of a polymer/nanoparticle solution, which is the x-axis in the Figure, corresponds to the x-axis of **Figure 5.3**; for instance, a concentration of 0.5 wt. % of polymer/nanoparticle solution corresponded to a concentration of 4 wt. % of nanoparticles for short composite nanofibers. The viscosity of the polymer/nanoparticle solutions gradually increased as the nanoparticle concentration was increased. However, the added-nanoparticle-concentration threshold (5 wt. %) that amounted to a significant change in fiber length, as shown in **Figure 5.3**, was not related to the viscosity of the polymer/nanoparticle solution. These results

showed that the viscosity of the polymer/nanoparticle solutions did not determine the length of the short composite nanofibers.

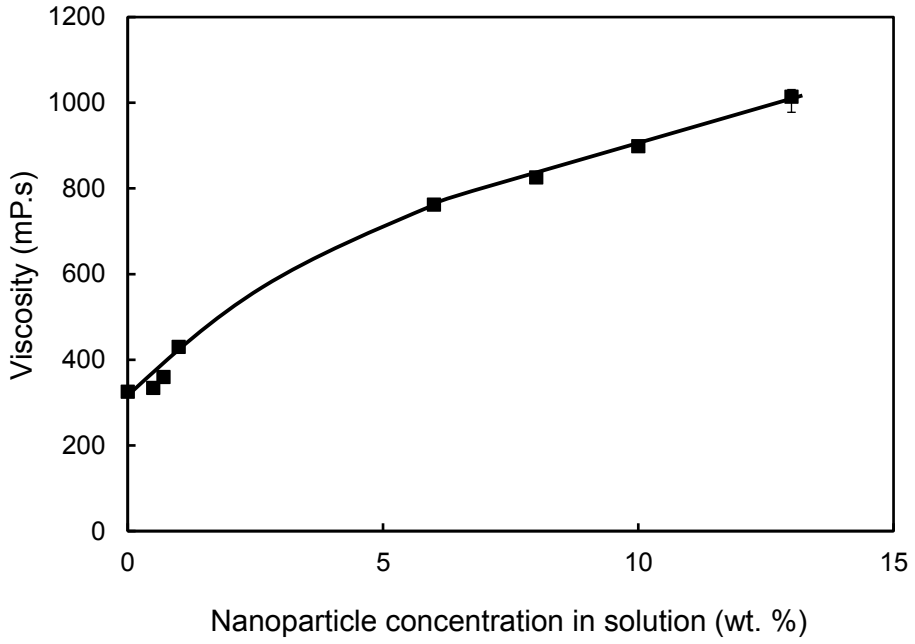

Figure 5.4. Viscosity of the polymer/nanoparticle solutions of various TiO_2 concentrations. The polymer concentration in the solutions was 13 wt. %.

5.3.2. The effect of the zeta potential of nanoparticles on composite nanofiber length

The dispersion conditions of the nanoparticles in the polymer nanofibers were an important parameter, and the length of the short composite nanofibers might have been related to the dispersion conditions. Veronovsky et al. have reported that the dispersion condition of TiO_2 was affected by its zeta potential [31]. Therefore, in order to confirm the effect of the dispersion of TiO_2 on the length of short composite nanofibers, the zeta potential of TiO_2 nanoparticles in the solution was controlled by changing the pH of the solution. **Figure 5.5** shows the zeta potentials of TiO_2 nanoparticles dispersed in the deionized water at various pHs. The zeta potentials of the nanoparticles were gradually decreased from 25 to -34 mV with an increase in the pH of the solution. The pH of the

polymer/nanoparticle solutions was approximately 6.5, so the short composite nanofibers shown in **Figures 5.1-3** were fabricated from a solution with nanoparticles with a zeta potential of approximately -5 mV. In order to change the dispersion conditions of the nanoparticles in solution, polymer/nanoparticle solutions with pH values of 4 and 9 were prepared, and these contained nanoparticles with zeta potentials of 17 and -29 mV, respectively. The zeta potentials of cellulose acetate polymer were -7 and -17 mV at pH values of 4 and 9, respectively [32]. Therefore, the nanoparticles in solution at pH 9 were well dispersed (nanoparticles: -29 mV, polymer: -17 mV), in contrast with agglomerate conditions in the solution at pH 4 (nanoparticles: 17 mV, polymer: -7 mV).

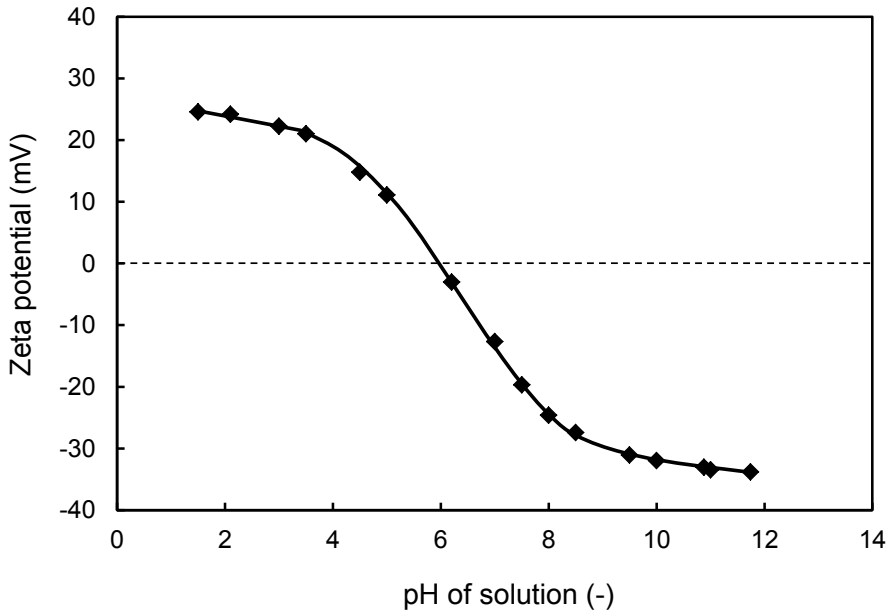

Figure 5.5. Zeta potential of TiO_2 nanoparticles in solution at various values for pH.

In order to investigate the effect of the zeta potential of the nanoparticles in short composite nanofibers, the morphologies of short composite nanofibers with a 4 wt. % concentration of nanoparticles fabricated from polymer/nanoparticles solution at various

values of pH were observed. **Figure 5.6** shows the short composite nanofibers with a 4 wt. % concentration of nanoparticles fabricated from a polymer/nanoparticle solution with pH values of 4 and 9. The short composite nanofibers fabricated from a polymer/nanoparticle solution at pH 4 had a few beads, and branched fibers were recognized (**Figure 5.6a**). On the other hand, the short composite nanofibers fabricated from a polymer/nanoparticle solution at pH 9 had a smooth surface, and no beads were observed (**Figure 5.6b**). These results showed that nanoparticles were locally agglomerated at pH 4, and nanoparticles were well dispersed at pH 9.

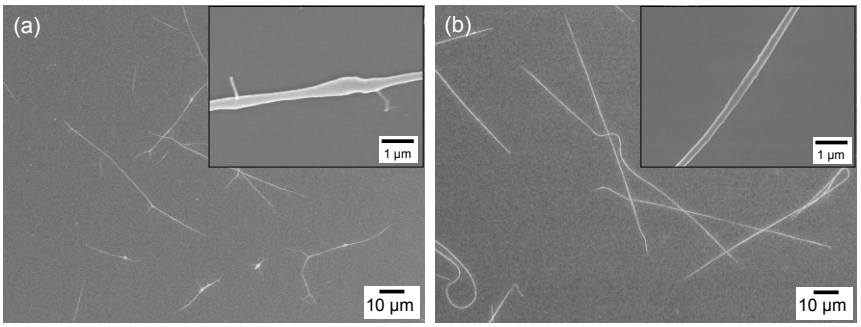

Figure 5.6. Short composite nanofibers with a 4 wt. % concentration of nanoparticles fabricated from a polymer/nanoparticle solution at pH 4 (a) and pH 9 (b).

The effect of zeta potential on the length of short composite fibers was further confirmed for nanoparticle concentrations of 4 to 38 wt. % at pH values of 4 to 9. **Figure 5.7** shows the relationship between the average length of short composite nanofibers and various nanoparticle concentrations and pH values of a polymer/nanoparticle solution. The average lengths of short composite nanofibers with nanoparticle concentrations of 4 and 5 wt. % were increased as the pH of the solution was increased; in other words, there was a decrease in the zeta potential of the nanoparticles in the solution. On the other hand, the average length of short composite nanofibers with nanoparticle concentrations of 7 and 38 wt. % did not change when the

pH of the solution was changed, which means the zeta potential of the nanoparticles had not changed. These results indicated that the surface charges of the nanoparticles in the polymer/nanoparticle solution affected the average length of the short composite nanofibers only at low nanoparticle concentrations of 4 and 5 wt. %.

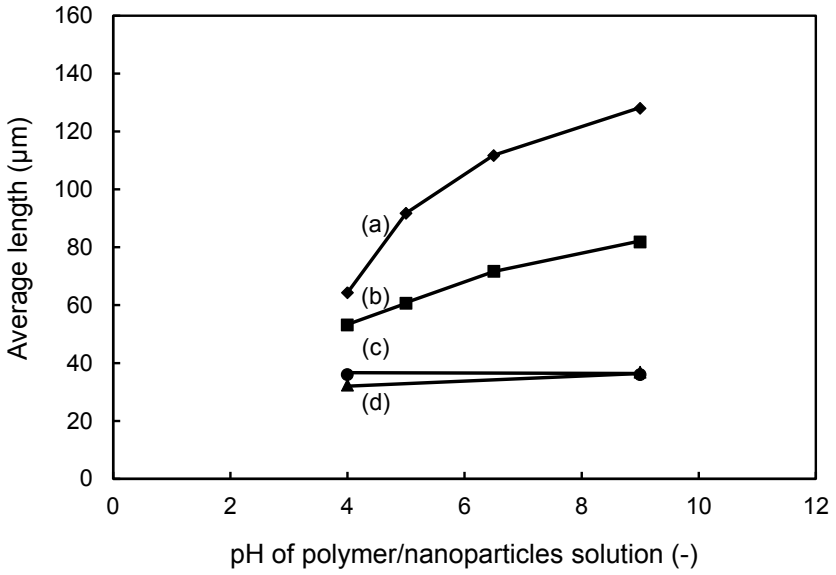

Figure 5.7. Average length of a short composite nanofiber with nanoparticle concentrations of 4 wt. % (a), 5 wt. % (b), 7 wt. % (c), and 38 wt. % (d) polymer/nanoparticle solutions at various values for pH.

5.3.3. Fabrication mechanism of short composite nanofibers

In order to discuss the mechanism of the fabrication of short composite nanofibers, the conditions of the electrospinning jets of the polymer/nanoparticle solutions were observed for different nanoparticle concentrations and values of pH. **Figure 5.8** shows the solution jet of a polymer/nanoparticle solution at pH 6.5 during the fabrication of short composite nanofibers with a 4 wt. % concentration of nanoparticles. There were no differences between the conditions of the electrospinning jets of polymer/nanoparticle solutions at various concentrations and values of pH. The electrospinning jet in the fabrication of short composite nanofibers was initially straight

and continuous, and then it was broken and spread-out several millimeters away from the needle tip with a spread angle of approximately 20^{o}. The electrospinning jet in the fabrication of short composite nanofibers was different from the electrospinning jet in the fabrication of continuous nanofibers, which was not spread and spiral at 1 to 2 cm away from the needle tip [33].

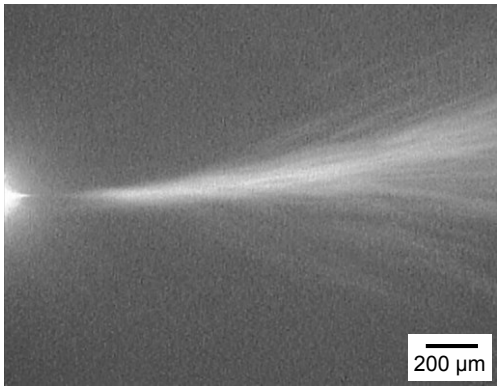

Figure 5.8. Electrospinning jet of a polymer/nanoparticle solution at pH 6.5 during the fabrication of short composite nanofibers with a 4 wt. % concentration of nanoparticles.

Figure 5.9 shows a short composite nanofiber with a 4 wt. % concentration of nanoparticles fabricated from a solution at pH 9. **Figure 5.9b** shows the end portion of a short composite nanofiber, which corresponds to the rectangle in **Figure 5.9a**. The diameter at the end portion of the short composite nanofiber was narrower than the diameter of the center portion. The narrower diameter at the end portion of the short composite nanofiber was observed on all the prepared short composite nanofibers. This indicated that the composite fiber was locally stretched by the electric field generated from the applied high voltage, and led to a thinning of the diameter of the composite nanofiber and to a breakaway of the composite nanofiber.

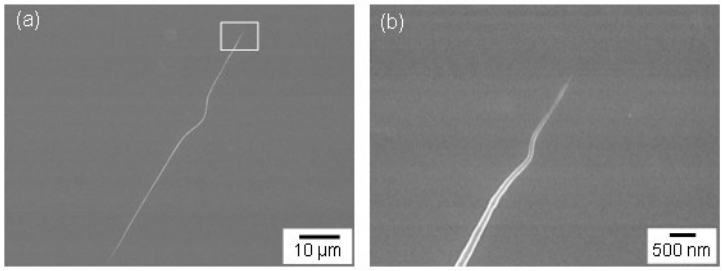

Figure 5.9. A short composite nanofiber with a 4 wt. % concentration of nanoparticles (a), and the end portion of the nanofiber (b). The pH of the polymer/nanoparticle solution is 9.

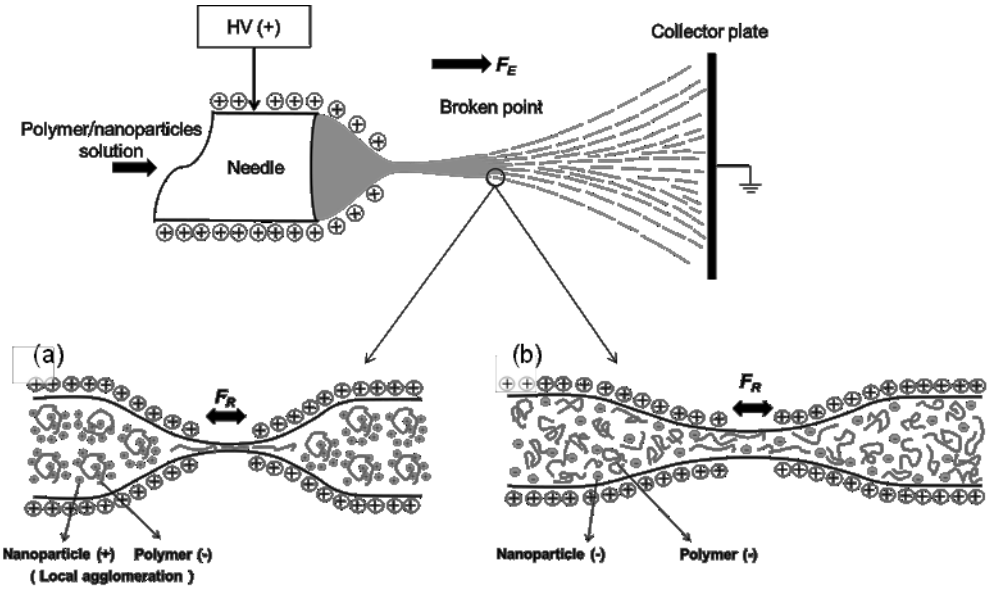

Figure 5.10. Fabrication mechanism of short composite nanofibers with a polymer/nanoparticle solution at pH 4 (a) and pH 9 (b).

Based on the observation of short composite nanofibers, a mechanism for the fabrication of a short composite nanofiber was proposed, and is shown in **Figure 5.10**. A positive high voltage generated both the electric field, $\boldsymbol{F_E}$, between the needle tip and the collector plate, and the positive charges on the surface of the polymer/nanoparticle solution. The electrospinning jet for the polymer/nanoparticles solutions was stretched and made thinner due to the repulsive force, $\boldsymbol{F_R}$, which was generated between the

positive charges on the surface of the polymer/nanoparticle solutions. At low concentrations of nanoparticles in a solution at pH 4, the positively charged nanoparticles were attracted to the negatively charged polymer, and they were locally aggregated. Thus, the solution was easily broken during stretching, which resulted in a short length (**Figure 5.10a**). On the other hand, at a low concentration of nanoparticles in solutions at pH 9, the polymers were repelled by the negatively charged nanoparticles, and, thus, the nanoparticles were evenly dispersed in the solution and the composite nanofiber became longer (**Figure 5.10b**). The negative charges within the polymer/nanoparticle solution were attracted to the positive charges generated on the surface of the polymer/nanoparticle solution and then redistributed to allow the electric field inside the electrified polymer/nanoparticles solution to be zero. This mechanism has been proposed by Reneker et al. in the electrospinning of various polymer solutions [34]. With a high concentration of nanoparticles, either positively or negatively charged nanoparticles were locally aggregated with the polymer, and then composites nanofibers were easily cut, which resulted in shorter composite nanofibers. Thus, the surface charges of the nanoparticles affected the length of the short composite nanofibers only at low concentrations of nanoparticles.

5.4. Conclusions

Short polymer/nanoparticle composite fibers with concentrations of nanoparticles as high as 50 wt. % were successfully fabricated via electrospinning using 13 wt. % cellulose acetate polymer under a voltage of 5.5 kV and at a flow rate of 0.1 μL/min. The concentration and the surface charges of nanoparticles affected the length of short composite nanofibers. The average lengths of short composite nanofibers were

significantly decreased from 112 to 70 μm with an increase in the nanoparticle concentration of as much as 5 wt. %, and further increases in nanoparticle concentration resulted in a more gradual decrease (from 60 to 40 μm). The lengths of short composite nanofibers with low concentrations of nanoparticles were affected by the surface charge of the nanoparticles. Longer composite nanofibers were fabricated from solutions containing negatively charged nanoparticles, and shorter composite nanofibers were fabricated from solutions containing positively charged nanoparticles. The negatively charged nanoparticles were more evenly dispersed to the negatively charged polymer in the solution, which resulted in an elongation of the fabricated composite nanofibers. At high concentrations of nanoparticles, nanoparticles with either positive charges or negative charges were locally aggregated with the polymer, which allowed the composite nanofibers to be easily cut resulting in shorter composite nanofibers.

5.5. References

[1] L. Francis, F. Giunco, A. Balakrishnan, E. Marsano, Synthesis, characterization and mechanical properties of nylon–silver composite nanofibers prepared by electrospinning, Curr. Appl. Phys. 10 (2010) 1005-1008.

[2] R. Nirmala, K.S. Jeon, B.H. Lim, R. Navamathapan, H.Y. Kim, Preparation and characterization of copper oxide particles incorporated polyurethane composite nanofibers by electrospinning, Ceram. Int. 39 (2013) 9651-9658.

[3] J.S. Im, S.J. Park, T. Kim, Y.S. Lee, Hydrogen storage evaluation based on investigations of the catalytic properties of metal/metal oxides in electrospun carbon fibers, Int. J. Hydrog. Energy 34 (2009) 3384-3388.

[4] E. Zhao, C. Ma, W. Yang, Y. Xiong, J. Li, J. Sun, Electrospinning $La_{0.8}Sr_{0.2}Co_{0.2}Fe_{0.8}O_{3-\delta}$ tubes impregnated with $Ce_{0.8}Gd_{0.2}O_{1.9}$ nanoparticles for an intermediate temperature solid oxide fuel cell cathode, Int. J. Hydrog. Energy 38 (2013) 6821-6829.

[5] S. Anita, B. Brabu, D. J. Triruvadigal, C. Gopalakrishnan, T.S. Natarajan, Optical, bactericidal and water repellent properties of electrospun nano-composite membranes of cellulose acetate and ZnO, Carbohydr. Polym. 87 (2012) 1065-1072.

[6] V. Modafferi, G. Panzera, A. Donato, P.L. Antonucci, C. Cannilla, N. Donato, D. Spadaro, G. Neri, Highly sensitive ammonia resistive sensor based on electrospun V_2O_5 fibers, Sens. Actuator B: Chem.163 (2012) 61-68.

[7] A. Mahapatra, B.G. Mishra, G. Hota, Electrospun Fe_2O_3-Al_2O_3 nanocomposite fibers as efficient adsorbent for removal heavy metal ions from the aqueous solution, J. Hazard. Mater. 258-259 (2013) 116-123.

[8] G. Yu, X. Li, X. Cai, W. Cui, S. Zhou, J. Weng, The photoluminescence enhancement of electrospun poly(ethylene oxide) fibers with CdS and polyaniline inoculations, Acta Materialia 56 (2008) 5775-5782.

[9] L. Huang, L. Cheng, H. Yu, J. Zhang, L. Zhou, J. Sun, H. Zhong, X. Li, Y. Tian, Y. Zheng, T. Yu, C. Li, H. Zhong, W. Liu, L. Zhang, J. Wang, B. Chen, Electrospinning preparation and optical transition properties of $Eu(DBM)_3Phen$/PS fluorescent composite fibers, Opt. Commun. 285 (2012) 1476-1480.

[10] H.R. Pant, D.R. Pandeya, K.T. Nam, W. Baek, S.T. Hong, H.Y. Kim, Photocatalytic and antibacterial properties of a TiO_2/nylon-6 electrospun nanocomposite mat containing silver nanoparticles, J. Hazard. Mater. 189 (2011) 465-471.

[11] R. Liu, H. Ye, X. Xiong, H. Liu, Fabrication of TiO_2/ZnO composite nanofibers by electrospinning and their photocatalytic property, Mater. Chem. Phys. 121 (2010) 432-439.

[12] H.R. Pant, B. Pant, P. Pokharel, H.J. Kim, L.D. Tijing, C.H. Park, D.S. Lee, H.Y. Kim, C.S. Kim, Photocatalytic TiO_2–RGO/nylon-6 spider-wave-like nano-nets via electrospinning and hydrothermal treatment, J. Membr. Sci. 15 (2013) 225-234.

[13] Y. Horie, T. Watanabe, M. Deguchi, D. Asakura, T. Nomiyama, Enhancement of carrier mobility by electrospun nanofibers of Nb-doped TiO_2 in dye sensitized solar cells, Electrochim. Acta, 105, (2013) 394-402.

[14] J.S. Lee, Y.I. Lee, H. Song, D.H. Jang, Y.H. Choa, Synthesis and characterization of TiO_2 nanowires with controlled porosity and microstructure using electrospinning method, Curr. Appl. Phys. 11 (2011) S210-S214.

[15] M. Su, J. Wang, H. Du, P. Yao, Y. Zheng, X. Li, Characterization and humidity sensitivity of electrospun ZrO_2:TiO_2 hetero-nanofibers with double jets, Sens. Actuators B: Chem. 161 (2012) 1038-1045.

[16] L. Zhou, N. Wu, Q. Cao, B. Jing, X. Wang, Q. Wang, H. Kuang, A novel electrospun PVDF/PMMA gel polymer electrolyte with in situ TiO_2 for Li-ion batteries, Solid State Ionics 249-250 (2013) 93-97.

[17] X. Zhang, S. Xu, G. Han, Fabrication and photocatalytic activity of TiO2 nanofiber membrane, Mater. Lett. 63(2009) 1761-1763.

[18] M. Hamadanian, A. Akbari, V. Jabbari, Electrospun titanium dioxide nanofibers: fabrication, properties and its application I photo-oxidative degradation of methyl orange (MO), Fibers Polym. 12 (2011) 880-885.

[19] A. Wagh, et al, A short circulating peptide nanofiber as a carrier for tumoral delivery, Nanomedicine: NBM 9 (2013) 449-457.

[20] L. Fu, Y. Wu, F. Li, B. Zhang, Synthesis of $InNbO_4$ short nanofiber membrane as visible-light-driven photocatalyst, Mater. Lett. 109 (2013) 225-228.

[21] S. Jiang, G. Duan, J. Schöbel, S. Agarwal, A. Greiner, Short electrospun polymeric nanofibers reinforced polyimide nanocomposites, Compos. Sci. Technol. 88 (2013) 57-61.

[22] M.H. Al-Saleh, U. Sundararaj, Review of mechanical properties of carbon nanofiber/polymer composites, Composites: Part A 42 (2011) 2126-2142.

[23] M. Endo, Y.A. Kim, T. Hayashi, K. Nishimura, T. Matusita, T. Mayashita, M.S. Dresselhaus, Vapor-grown carbon fiber (VGCFs) basic properties and their battery applications, Carbon 39 (2001) 1287-1297.

[24] S. Mahalingam, M. Edirisinghe, Forming of polymer nanofibers by a pressurised gyration process, Macromol. Rapid Commun. 34 (2013) 1134–1139.

[25] L.D. Tijing, A. Amarjargal, Z. Jiang, M.T.G. Ruelo, C.H. Park, H.R. Pant, D.W. Kim, D.H. Lee, C.S. Kim, Antibacterial tourmaline nanoparticles/polyurethane hybrid mat decorated with silver nanoparticles prepared by electrospinning and UV photo reduction, Curr. Appl. Phys. 13 (2013) 205-210.

[26] N.A.M. Barakat, M.F. Abadir, F.A. Sheikh, M.A. Kanjwal, S. J. Park, H.Y. Kim, Polymeric nanofibers containing solid nanoparticles prepared by electrospinning and their applications, Chem. Eng. 156 (2010) 487-495.

[27] D.P. Macwan, P.N. Dave, S. Chaturvedi, A review on nano-TiO_2 sol–gel type syntheses and its applications, J. Mater. Sci. 46 (2011) 3669–3686.

[28] A.E. Deniz, A. Celebioglu, F. Kayaci, T. Uyar, Electrospun polymeric nanofibrous composites containing TiO_2 short nanofibers, Mater. Chem. Phys. 129 (2011) 701-704.

[29] I.W. Fathona, A. Yabuki, One-step fabrication of short electrospun fibers using an electric spark, J. Mater. Proces. Technol. 213 (2013) 1894-1899.

[30] I.W. Fathona, A. Yabuki, A Simple One-Step Fabrication of Short Polymer Nanofibers via Electrospinning, J. Mater. Sci. 49 (2014) 3519–3528.

[31] N. Veronovski, P. Andreozzi, C. La Mesa, M.S. Smole, Stable TiO_2 dispersions for nanocoating preparation, Surf. Coat. Tech. 204 (2010) 1445-1451.

[32] H. Matsumoto, Y. Koyama, A. Tanioka, Preparation and characterization of novel weak amphoteric charged membrane containing cysteine residues, J. Coll. Interface Sci. 239 (2001) 467–474.

[33] D.H. Reneker, A.L. Yarin, H. Fong, S. Koombhongse, Bending instability of electrically charged liquid jet of polymer solutions in electrospinning, J Appl. Phys. 87 (2000) 4531-4547.

[34] D.H. Reneker, A.L. Yarin, Electrospinning jets and polymer nanofibers, Polymer 49 (2008) 2387-2425.

Chapter 6

Summary

The one-step fabrication method to fabricate short polymer fiber by electrospinning has been discussed. The effect of electrospinning parameters such as polymer concentration, applied voltage, and solution flow rate, and nanoparticle addition have been investigated in order to control the length of short polymer fiber.

Two types of one-step fabrication processes for short polymer fibers by electrospinning were developed, which is used electric spark as cutting tool and is controlled electrospinning conditions. The methodology to control the length of short polymer fibers was developed by altering a needle inner diameter, applied voltage, flow rate of polymer solution, and added the nanoparticles. These one-step fabrication processes and methodology in controlling short polymer fiber could be simply explained in the following:

(i) The one-step fabrication process was combining an electrospinning method and electric spark generation at once time. Electric spark was used as a cutting tool of electrospun polymer fiber during electrospinning process. High voltage with a square wave was applied to two electrodes to generate a periodic electric spark that could be recognized at 4.1 kV. The following results has been discussed and explained in Chapter 2:

   a. Solution of cellulose acetate and organic solvent was ejected from a syringe needle and was stretched by the electric field then it cut after passed through the gap between the tips of two electrodes that generated an electric spark with frequency of 5 kHz.

b. The short fibers of average 231 μm were found on the collector plate with a density of 1-5 fibers per 0.12x0.2 mm^2, whereas the fibers that did not flow through to the electric spark were uncut and remained as continuous fibers on the collector plate.

c. The theoretical fiber length was calculated at 271 μm when employing a 5 kHz of electric spark, which was in good agreement with the length of the short fibers obtained in the experiment.

(ii) The simple and one-step process fabrication of short polymer nanofibers has been successfully developed based on simple electrospinning method. The length also could be controlled by controlling electrospinning parameters. The process of this methodology is described in Chapter 3, which could be summarized as follows:

a. A polymer solution was loaded into a syringe, and was then ejected by the application of high voltage. The effect of the concentration of the polymer solution, the applied voltage, and the flow rate of the polymer solution was investigated for its effect on the length of short nanofibers.

b. The concentration of the cellulose acetate polymer in the solution was important factor which varied from 13 to 15 wt. %. The length of fibers was increased by increasing the flow rate of the solution, and it was decreased with an increase in applied voltage, resulting in controllable length of short nanofibers at 37 to 670 μm.

c. The edges of the short nanofibers were narrowed by stretching. Observation of the polymer solution jet that was ejected from the needle tip showed it passing straight, and then spreading due to lateral perturbations on its surface.

The breaking of the fibers into short nanofibers occurred because the repulsive force from the surface charges and the longitudinal force from the applied voltage surpassed the tensile strength of the polymer solution jet.

(iii) The effect of the needle size on the length of nanofiber was investigated and describe in Chapter 4, and the following results were obtained: The short nanofiber average diameter was increased approximately twice, as the needle inner diameter was increased from 0.16 to 0.26 mm. The short nanofibers average length was increased with the factors 1.5-1.6×, as needle inner diameter was increased 1.6×. The breaking of the fibers into short nanofibers occurred due to an imbalance between the force of the surface tension of the polymer solution and the longitudinal force from the applied voltage.

(iv) The effect of nanoparticle concentration and surface charge on short composite fibers fabrication has been investigated (Chapter 5) resulted in the following points:

a. Short composite fiber has been fabricated via electrospinning using 13 wt. % cellulose acetate polymer and TiO_2 nanoparticles under a voltage of 5.5 kV and at a flow rate of 0.1 μL/min. Concentration of nanoparticle in the fiber could be achieved as high as 50 wt. %.

b. The average lengths of short composite nanofibers were significantly decreased from 112 to 70 μm with an increase in the nanoparticle concentration of as much as 5 wt. %, and further increases in nanoparticle concentration resulted in a more gradual decrease (from 60 to 40 μm).

c. The lengths of short composite nanofibers with low concentrations of nanoparticles were affected by the surface charge of the nanoparticles.

Longer composite nanofibers were fabricated from solutions containing negatively charged nanoparticles, and shorter composite nanofibers were fabricated from solutions containing positively charged nanoparticles. The negatively charged nanoparticles were more evenly dispersed to the negatively charged polymer in the solution, which resulted in an elongation of the fabricated composite nanofibers.

d. At high concentrations of nanoparticles, nanoparticles with either positive charges or negative charges were locally aggregated with the polymer, which allowed the composite nanofibers to be easily cut resulting in shorter composite nanofibers.